INVESTIGATING THE MECHANISM OF PROTEIN SURFACE IMPRINTING THROUGH MINIEMULSION POLYMERISATION

SHALOM WANGRANGSIMAKUL
(B.Eng.(Hons.), NUS)

A THESIS SUBMITTED

FOR THE DEGREE OF MASTER OF ENGINEERING

DEPARTMENT OF CHEMICAL AND BIOMOLECULAR ENGINEERING

NATIONAL UNIVERSITY OF SINGAPORE

2009

Acknowledgements

I would like to thank Dr. Tong Yen Wah for his patience and guidance for the past 3 years. In my undergraduate days, I only remembered him as the-guy-who-taught-us-about-radiation but now, as I leave NUS, he will be remembered as a supervisor who genuinely cares for his students. I could not have asked for a better supervisor.

I would like to thank Dr. Tan Chau Jin (known to us as Chaoren), my mentor, friend and a Manchester United fan. He has taught me so much about molecular imprinting, in theory as well as in the lab. It was a pleasure working with him in various projects and I wish him all the best in his career.

I would also like to thank all my lab mates in WS2-06-17; those who are currently sitting in the office and those who have already graduated. They have made the office and lab a pleasant place to work in and they will remain an important part of my life.

Finally, I would like to thank the admin officers of E5-02 and the lab officers of WS2-06 and E5-04. They were very friendly and professional in their work and they have made my graduate life enjoyable.

Table of contents

Acknowledgements i

Table of contents ii

Summary vi

List of tables viii

List of figures ix

Nomenclature xi

Chapter 1 Introduction 1

Chapter 2 Literature review 4

2.1 Molecular recognition 4

2.2 Molecular imprinting 6

2.2.1 Advantages of MIPs 8

2.2.2 Types of molecular imprinting 8

2.2.2.1 Covalent 9

2.2.2.2 Non-covalent 10

2.2.2.3 Sacrificial-spacer 13

2.2.3 MIP beads 15

2.3 Imprinting of proteins 16

2.3.1 Challenges in protein imprinting 17

2.3.2 Surface imprinting 19

2.3.3 Template immobilisation 21

Chapter 3 Optimising the preparation of protein surface-imprinted nanoparticles 24

3.1 Introduction 24

3.2 Preparation of protein surface-imprinted nanoparticles via miniemulsion polymerisation 25

3.2.1 Template: Ribonuclease A 25

3.2.2 Functional monomer: Methyl methacrylate 26

3.2.3 Cross-linker: Ethylene glycol dimethacrylate 28

3.2.4 Miniemulsion polymerisation 28

3.2.5 Factorial design 30

3.3 Experimental section 31

3.3.1 Materials 31

3.3.2 Preparation of BSA-imprinted nanoparticles 32

3.3.3 Preparation of non-imprinted nanoparticles 34

3.3.4 Batch rebinding tests 35

3.3.5 Determination of the swelling ratio 37

3.3.6 Determination of the particle size using field-emission scanning microscope 37

3.4 Results and discussion 38

3.4.1 Size and morphology of the MIPs and NIPs 38

3.4.2 Batch rebinding tests 42

3.5 Conclusion 46

3.5.1 Summary 46

3.5.2 Recommendations 47

Chapter 4 Investigating protein-surfactant interactions in the preparation of protein surface-imprinted nanoparticles 48

4.1 Introduction 48

4.2 Experimental section 49

4.2.1 Materials 49

4.2.2 Preparation of RNase A, BSA- and Lys-imprinted and non-imprinted nanoparticles 49

4.2.3 Elemental analysis 51

4.2.4 Determination of morphological features 51

4.2.5 Batch rebinding tests 51

4.2.6 Competitive batch rebinding tests 52

4.2.7 Kinetics study 54

4.2.8 Desorption study 54

4.2.9 CD study 55

4.3 Results and discussion 55

4.3.1 Size and morphology of the MIPs and NIPs 55

4.3.2 Elemental analysis 59

4.3.3 Batch rebinding tests 59

4.3.4 Competitive batch rebinding tests 62

4.3.5 Rebinding kinetics 65

4.3.6 Desorption study 66

4.3.7 Protein-surfactant interactions and their effects on the imprinting efficiency 68

4.4 Conclusions 74

Chapter 5 Conclusions 76

5.1 Determining the principal factors which affect the imprinting efficiency 76

5.2 Investigating protein-surfactant interactions and their role in successful imprinting 77

5.3 Suggestions for future work 78

5.3.1 Further investigation on the protein-surfactant interaction 78

5.3.2 Modification of the BSA to improve its interaction with the surfactant micelle 79

Bibliography 80

Appendix A: List of publications 93

Summary

Molecular recognition can be described as the specific interaction between two or more molecules by non-covalent means. Such interactions can be seen in the human body where they play an important role in vital biological functions. The ability to selectively recognise and bind to specific molecules is also useful for various commercial and industrial applications. As a result, numerous artificial systems which possess molecular recognition have been developed.

Molecular imprinting is a well-established technique to create synthetic binding sites on a polymer matrix. Not only can the resulting imprinted polymer specifically recognise pre-determined target molecules, they also possess favourable physical and chemical properties, such as good mechanical strength, and the ability to withstand wide temperature and pH ranges. Traditionally, molecular imprinting has been widely used to create synthetic receptors for smaller molecules but limited success has been achieved for larger molecules such as proteins.

In this work, we have synthesised protein-imprinted nanoparticles using miniemulsion polymerisation, with methyl methacrylate and ethylene glycol dimethacrylate as the functional and cross-linking monomers, respectively. Initially, ribonuclease A was chosen as the template protein and the nanoparticles showed high molecular selectivity for the protein. However, when bovine serum albumin or lysozyme was used as the template, molecular recognition was not successfully achieved. The latter part of the work was

focused on understanding the mechanism involved during the imprinting in order to explain why molecular imprinting was achieved with varying success depending on the template protein.

List of tables

Table 3.1a Half-fraction factorial design table with three factors (A, B, and C) and four treatments (T2, T3, T5, and T8). +/- represents the high and low levels, respectively. 31

Table 3.1b Values of the high and low levels (+/-) for the three factors. 31

Table 3.2a Variation of the three factors across the four treatments. 32

Table 3.2b Composition of the first aqueous phase. 32

Table 3.2c Composition of the second aqueous phase. 33

Table 3.2d Amount of initiators. 33

Table 3.3 Preparation of stock solution for the batch rebinding test of one set of MIP. 35

Table 4.1a Composition of the oil phase. 50

Table 4.1b Composition of the first aqueous phase. 50

Table 4.1c Composition of the second aqueous phase. 50

Table 4.1d Amount of initiators. 50

Table 4.2 Results of the Elemental Analysis. 59

Table 4.3 Calculated separation factors of the NIP and RMIP nanoparticles based on the competitive binary rebinding test. 64

Table 4.4 Results of the desorption study using different solvents. 67

List of figures

Figure 2.1 Schematic of the molecular imprinting technique. 7

Figure 2.2 Schematic of: A) Non-covalent imprinting B) Covalent imprinting. 12

Figure 2.3 Imprinting 2,3,7,8-tetrachlorodibenzodioxin (TCDD) via the sacrificial-spacer approach. 14

Figure 3.1 Ribbon diagram of RNase A showing the Tyr residues and the disulphide bonds. 26

Figure 3.2 Structure of methyl methacrylate (MMA). 27

Figure 3.3 Structure of ethylene glycol dimethacrylate (EGDMA). 28

Figure 3.4 Polymerisation reactor setup. 34

Figure 3.5 FESEM images of: (A) MIPs and (B) NIPs under treatment T2. 39

Figure 3.6 Diameter of the nanoparticles from the four treatments. 40

Figure 3.7 Swelling ratios of the nanoparticles from the four treatments. 42

Figure 3.8 Batch rebinding tests of BSA for MIP and NIP of the 4 treatments. 43

Figure 4.1 FESEM images of: (A) NIP, (B) BMIP, (C) RMIP, and (D) LMIP. 58

Figure 4.2 Results of batch rebinding tests in: (A) RNase A, (B) BSA, and (C) Lys protein solutions. 62

Figure 4.3 Results of the binary protein competitive batch rebinding test. 63

Figure 4.4 Results of the ternary protein competitive batch rebinding test. 65

Figure 4.5 RNase A adsorption profiles of the NIP and RMIP nanoparticles. 66

Figure 4.6 (a) Adsorption of template protein molecule to the micelle; (b) molecular imprinting on the surface of the nanoparticles; (c) removal of the template RNase A molecules frees the imprinted cavities. 69

Figure 4.7 Solvent-corrected CD spectra of BSA in different types of surfactant systems, illustrating the lack of protein-surfactant interaction. 72

Figure 4.8 Solvent-corrected (A) near-UV and (B) far-UV CD spectra of Lys, illustrating the change in the protein structure in the presence of surfactants. 73

Figure 4.9 Solvent-corrected far-UV CD spectra of RNase A in surfactant solutions, illustrating an optimum level of protein-surfactant interaction for protein imprinting through miniemulsion polymerisation. 74

Nomenclature

Abbreviations:

ACN	Acetonitrile
BET	Brunauer-Emmett-Teller
BMIP	Bovine serum albumin-imprinted polymer
BSA	Bovine serum albumin
C_F	Final protein concentration
C_I	Initial protein concentration
C_p	Amount of ligand adsorbed
C_s	Free ligand concentration
CD	Circular dichroism
CMC	Critical micelle concentration
CVPC	Chloresteryl (4-vinyl) phenyl carbonate
Cys	Cysteine
DI	Deionised
DNA	Deoxyribonucleic acid
EGDMA	Ethylene glycol dimethacrylate
FESEM	Field-emission scanning electron microscope
HPLC	High-performance liquid chromatography
K_D	Static distribution coefficient
Lys	Lysozyme
LMIP	Lysozyme-imprinted polymer

m	Mass of the polymer in each aliquot
MAA	Methacrylic acid
MIP	Molecularly imprinted polymer
MMA	Methyl methacrylate
MW	Molecular weight
NIP	Non-imprinted polymer
pI	Isoelectric point
PVA	Poly (vinyl alcohol)
Q	Amount of protein adsorbed
RNA	Ribonucleic acid
RNase A	Ribonuclease A
RMIP	Ribonuclease A-imprinted polymer
SDS	Sodium dodecyl sulphate
SR	Swelling ratio
TCDD	2,3,7,8-tetrachlorodibenzodioxin
TFA	Trifluoroacetic acid
Tyr	Tyrosine
UV	Ultraviolet
v/v	Volume/volume percentage solution
W_{dry}	Dry weight
w/o	Water-in-oil
w/v	Weight/volume percentage solution
W_{wet}	Swollen weight

Special symbols:

α	Separation factor
β	Relative separation factor

Chapter 1

Introduction

The ability to recognise molecules of a specific nature and shape, or molecular recognition, is a vital part of many chemical and biological processes. Various examples of molecular recognition can be seen in the human body, for example: enzyme catalysis, immuno-response and ligand-receptor interaction. This phenomenon has led to the development of numerous artificial receptors which aim to mimic the affinity and specificities of biomolecules which are found in nature.

Molecular imprinting is one such solution involving the creation of binding sites on a polymeric matrix which are complementary to the targeted molecule. In the past decade, great advances have been made in this field and it has established itself as one of the most effective methods to create synthetic receptors. Other than their high binding selectivity, molecularly imprinted polymers (MIPs) offer many advantages over their biological counterparts. MIPs can withstand high temperature and pressure, they are stable under a wide range of pH, they are reusable and are relatively simple to prepare. While much success has been achieved for the imprinting of small molecules, the imprinting of proteins and other macromolecules remained a challenge. The complex and flexible structure of the protein poses problems such as incompatible polymerisation conditions, unfavourable rebinding kinetics, and non-homogeneity of the binding sites.

In 2007, Tan C.J. and Tong Y.W. published a work in Langmuir which provided an effective method for the synthesis of protein surface-imprinted nanoparticles. Ribonuclease A (RNase A) was used as the template protein and the imprinting was carried out via miniemulsion polymerisation with methyl methacrylate (MMA) and ethylene glycol dimethacrylate (EGDMA) as the functional monomer and the cross-linker, respectively. The protein surface-imprinted nanoparticles were uniform, spherical, highly monodispersed, and had an average diameter of approximately 40 nm. Molecular recognition was successfully achieved, and the resulting protein-imprinted nanoparticles showed a greater preference towards the target RNase A, relative to the non-imprinted polymer.

Tong's group had developed an efficient method that involved a simple one-step miniemulsion polymerisation and the resulting surface-imprinted nanoparticles possessed excellent selectivity, as well as favourable rebinding kinetics. The method is also suitable for industrial-scale production due to its good heat transfer. Another advantage of the method is the versatility of the nanoparticles to be used in a wide range of applications due to their size and uniformness. As a result, it is of great interest to continue investigating this method in order to obtain a deeper understanding of the imprinting process which occurs during the miniemulsion polymerisation.

Hypothesis:

Tan's method of one-step miniemulsion polymerisation imprinting could be used to synthesise nanoparticles with the ability to recognise other proteins such as bovine serum albumin and lysozyme. It also hypothesised that the imprinting mechanism involves

interactions between the protein molecules and the monomer-encapsulated surfactant micelles.

Objectives:

In this research project, we aim to optimise the miniemulsion conditions of Tan's method in order to improve the selectivity of the nanoparticles and determine the factors which play an important role in determining the imprinting efficiency. Alternative proteins will also be used as the template. The latter part of this research will be focused on understanding the imprinting mechanism involved during the miniemulsion polymerisation and a study on the interaction between the proteins and the surfactant in the miniemulsion system will also be carried out.

Chapter 2

Literature Review

This literature review introduces the phenomenon of molecular recognition which is evident in the basic functions of our body and how molecular imprinting has been developed by science to imitate such process. The general principle of molecular imprinting and its three approaches: covalent, non-covalent, and sacrificial-spacer, are studied here. Greater emphasis is placed on non-covalent imprinting because it is the most common approach and is the approach adopted in this research project. The imprinting of proteins is then discussed, with its inherent challenges and difficulties, and various solutions that have been adopted by other research groups to circumvent them.

2.1 Molecular recognition

All important functions in the human body involve the specific recognition between biological molecules. For example: antibodies specifically bind to antigens to trigger the immune response, and transcription factors bind to a specific part of the DNA in the transfer of information to RNA. Understanding the interactions between these molecules and how they are able to specifically recognise each other is thus vital in order to gain a deeper understanding of the human body. Another example of specific recognition in the human body is the interactions between enzymes and substrates. Enzymes are proteins that catalyse various biochemical reactions and each enzyme is very specific in terms of the reaction it catalyses and the substrates involved in the reaction. They differ from

conventional catalysts because of their specificity which are highly dependent on the surrounding environment (e.g. temperature, pH). This enables them to distinguish between substrates which are in their correct shapes and those which are in a slightly altered form. The specificity is due to the presence of complementary geometric shapes in the enzymes which allow substrates to fit exactly into them. The first attempt to explain this phenomenon was Emil Fischer's 'lock and key' model in 1894. In this model, the enzyme acts as the lock and substrate as the key. Only the correct key, possessing a specific shape and size and having correctly positioned teeth, can fit in the keyhole and open the lock. Specific recognition is also present in many chemical processes outside the body, both in laboratories and chemical plants. For example: various bioassays in the development of new drugs, and host receptors on membranes used for the separation of specific compounds. Other areas which require specific recognition may include: catalysis, analytical chemistry, chemo- and biosensors. The ability to recognise molecules of a specific nature and shape, or molecular recognition, is thus a vital part of many biological and chemical processes. Whitcombe and Vulfson (2001) defined this phenomenon as 'the preferential binding of a chemical entity to a "receptor" with high selectivity over its close structural analogues'. There are many technologies that have been developed to create 'biomimics' that imitate the molecular recognition of biological molecules. Each technique has its own advantages and disadvantages, and molecular imprinting is one promising example with the potential to be used in a wide range of fields.

2.2 Molecular imprinting

The phenomenon of molecular recognition has challenged scientists to imitate this remarkable property which is so evident in our body. Synthetic receptors have been developed and these biomimics imitate the biological systems with their specific affinity and binding towards the target ligands. Molecular imprinting is an effective technique to create one such biomimic. Nicholls and Rosengren (2001) has precisely and concisely described molecular imprinting as 'a technique which involves the formation of binding sites in a synthetic polymer matrix that are of complementary functional and structural character to its "substrate" molecule'. The resulting product, or molecularly imprinted polymers (MIPs), are formed by the copolymerisation of the functional and cross-linking monomers in the presence of a template. In the pre-polymerisation mixture, the monomer and template are allowed to interact and a complex is formed between them. Depending on their nature, the interaction between the two can be covalent or non-covalent (Ye and Mosbach, 2008). Copolymerisation is then carried out with the cross-linker, which 'holds' the functional monomers in place, preserving the spatial orientations of the functional groups. Finally, the template is removed leaving behind binding sites which are complementary to the target molecule in terms of size, shape, and chemical functionality. These binding sites, with strong specific recognition for the template molecules, are then available for subsequent rebinding (Figure 2.1).

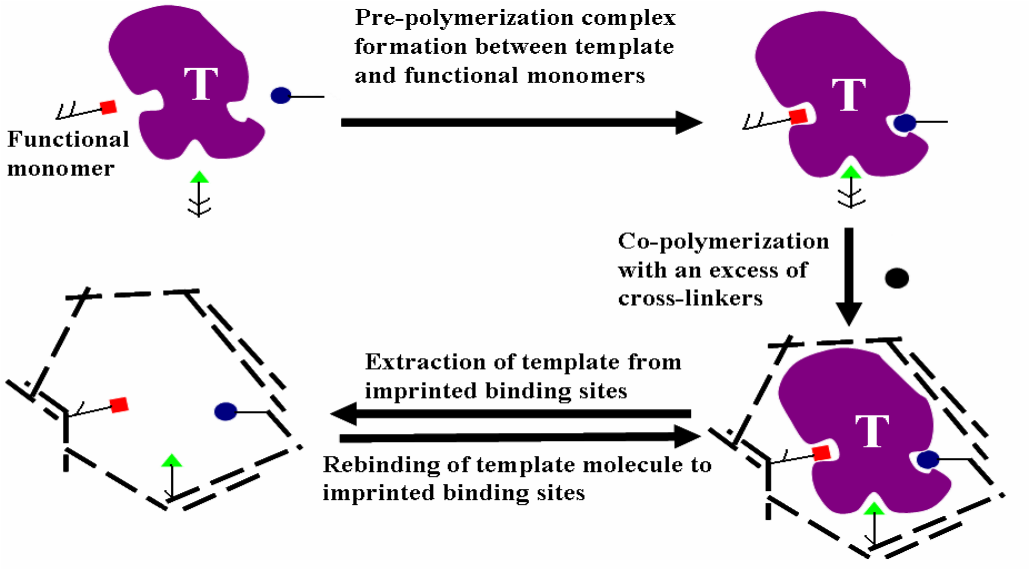

Figure 2.1 Schematic of the molecular imprinting technique.

Molecular imprinting has been used to produce synthetic receptors to target molecules of various nature and sizes. Great advancement and progress has been made for the imprinting of relatively small, low molecular weight and well-functionalised molecules such as sugars (Mayes et al., 1994; Parmpi and Kofinas, 2004; Sineriz et al., 2007), metal ions (Rao et al., 2006; Shirvani-Arani et al., 2008), amino acids (Reddy et al., 1999; Zhu and Zhu, 2008), and drugs (Alvarez-Lorenzo and Concheiro, 2004; Hiratani et al., 2007). However, less success has been achieved for larger entities, such as peptides and proteins (Kempe and Mosbach, 1995; Wulff, 2002; Turner et al., 2004 and 2006), cells (Dickert et al., 2001), viruses (Hayden et al., 2006), and bacteria (Hayden and Dickert, 2001). This is not surprising because for larger entities, the interaction between the template molecule and the functional monomers will be more complex which could lead to the formation of heterogeneous binding sites. Another difficulty encountered is the mass transfer limitation of the template molecules to the binding sites in the polymer matrix which would result in unfavourable rebinding kinetics (Pang et al., 2005). In this literature review, we will focus

on the imprinting of proteins, its limitations and challenges, and the progress and advancement in the field.

2.2.1 Advantages of MIPs

MIPs have many advantages compared to other synthetic biomolecule-based molecular recognition techniques: they have higher physical and chemical stability, and they are able to withstand a wider range of temperature, pH, and acid-base conditions without displaying a loss in molecular recognition (Nicholls and Andersson, 1995). MIPs are relatively simpler to prepare and therefore, are more cost-effective, and they can be prepared into forms suitable for the desired application, such as beads (Mayes and Mosbach, 1996; Lu et al., 2003; Say et al., 2003), membranes (Sergeyeva et al., 2003; El-Toufaili et al., 2004), and films (Piletsky et al., 1999; Miyahara and Kurihara, 2000). MIPs, being solid, also have a much higher physical strength and robustness than their biological counterparts, and can easily be separated from the rebinding mixture. Furthermore, their storage life is many years without the loss of affinity for the targeted molecule (Hillberg et al., 2005; Ramstrom et al., 1997). As a result, MIPs have great potential in various areas such as bioseparations, chemosensors, immunoassays, drug screening, and catalysis (Mahony et al., 2005).

2.2.2 Types of molecular imprinting

One of the most important considerations in the design of MIPs is the interaction which will occur between the functional monomer and the template. The choice of the monomer

will depend on the nature of the template as well as the environment in which the rebinding of the target molecule will be taking place (for example: aqueous or organic). Molecular imprinting is therefore classified into two main approaches according to the chemical bonds involved in the rebinding of the target molecule; covalent and non-covalent. Covalent imprinting was the main approach during the 1970s when MIPs were first being studied by Wulff's group (Sellergren, 2001). However, since its development in the 1980s by Mosbach's group, the non-covalent approach has become more common and it is the most widely used approach today (Sellergren and Allender, 2005). A third and less common type of imprinting is the sacrificial-spacer approach which combines the benefits of the previous two approaches (Whitcombe and Vulfson, 2001).

2.2.2.1 Covalent

In the covalent approach, a reversible covalent bond is formed between the functional monomer and the template (Figure 2.2B). Examples of these bonds are: ester, acetal/ketal, Schiff-base, and metal coordination (Takeuchi and Haginaka, 1999). The resulting template derivative is copolymerised with the cross-linker and the subsequent removal of the template requires cleavage of the covalent bonds using hydrolysis, for example (Whitcombe and Vulfson, 2001).

One of the advantages of this approach is that the stoichiometric ratio between the template and the monomer is determined, resulting in the homogeneity of the binding sites (Sellergren and Allender, 2005). The rebinding is also very selective and stable, since the binding cavities are an 'exact fit' (Whitcombe and Vulfson, 2001). However, the

rebinding kinetics of the MIPs is often not favourable due to the slow reformation of the covalent bonds and is therefore unsuitable for applications such as chromatographic separations. Another problem is that there are a limited number of covalent linkages available that can readily cleave and rebind (Takeuchi and Haginaka, 1999).

2.2.2.2 Non-covalent

In the non-covalent approach, the functional monomers complex with the template molecule through non-covalent interactions, such as electrostatic and hydrophobic interactions or hydrogen bonding (Figure 2.2A). The preparation of the complex is relatively easier since it only involves mixing the monomer with the template and the isolation of the resulting complex is not required. The rebinding kinetics of MIPs prepared by the non-covalent approach is also much more favourable and only mild conditions are required for the removal of the template molecule (Takeuchi and Haginaka, 1999). However, due to the weaker nature of the functional monomer-template interaction, the stability of the complex is lower, resulting in a lower concentration of the complex. The functional monomer is usually added in excess in order to obtain the maximum complex concentration but this may cause many different species of the complex to form in the polymerisation mixture. Consequently, the binding sites of the MIPs are no longer homogeneous in terms of affinity (Takeuchi and Haginaka, 1999).

One solution to this problem is the introduction of ‘second generation’ functional monomers which are able to bind much more strongly to specific functional groups on the template. Examples of the targeted groups are: carboxylates and phosphonates, carboxylic

acids, peptide backbones, amines and barbiturates (Whitcombe and Vulfson, 2001). Another popular solution is the template immobilisation method. In this method, the synthesis of the MIPs involves two distinct steps; template immobilisation, and polymerisation. First, the template molecules are immobilised covalently to a support and the polymerisation is subsequently carried-out, as usual, in the presence of the functional monomers and cross-linker. The benefits of this 2-step imprinting and its examples will be discussed further on in this review.

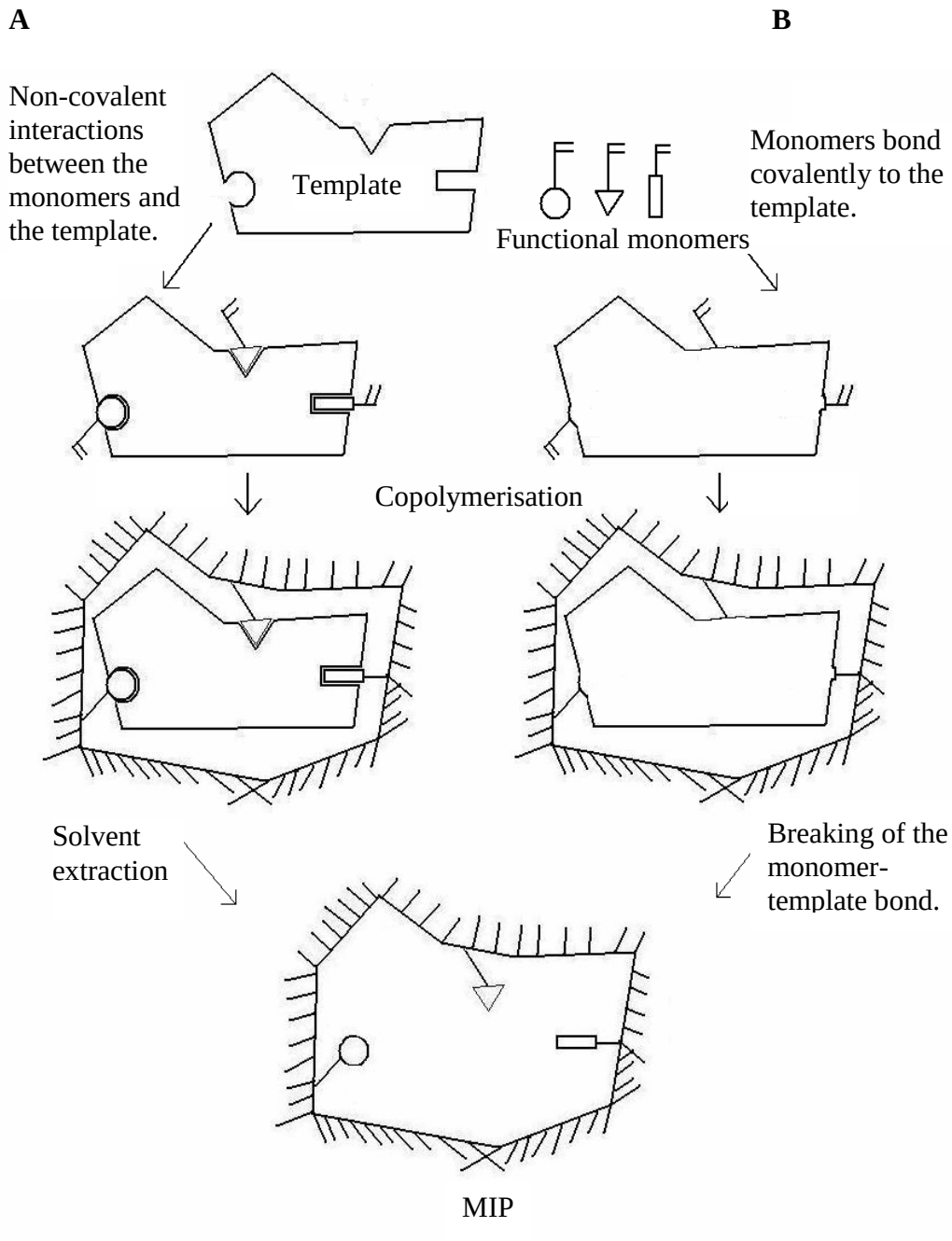

Figure 2.2 Schematic of: A) Non-covalent imprinting B) Covalent imprinting.

2.2.2.3 Sacrificial-spacer

This approach was introduced by Whitcombe et al. in 1995, which combined the advantages of covalent and non-covalent imprinting (Kandimalla and Ju, 2004; Whitcombe et al., 1995; Zhang and Ye, 2006). It relies on covalent bonding between the functional monomer and the template prior to polymerisation, and uses non-covalent interactions for the subsequent rebinding. This is possible due to the presence of a 'spacer' group on the monomer-template complex which is lost during the removal of the template, leaving behind a binding site available for non-covalent interactions. One of the advantages of this approach is that it is able to use weak hydrogen bonds during the rebinding of the imprinted molecule. This property is illustrated in the following example (Figure 2.3). Diurea is used as a template for the imprinting of 2,3,7,8-tetrachlorodibenzodioxin (TCDD) and two urea bridges act as sacrificial-spacers between the chlorine atom of the dioxin and the polymer-bound amine groups. During the template removal after copolymerisation, the 2,8-diamino-3,7-dichlorodibenzodioxin is removed by hydride reduction, leaving behind two amine groups bound to the polymer. These are then able to form hydrogen bonds with the chlorine atoms of the targeted TCDD during subsequent rebinding (Sellergren, 2001; Whitcombe and Vulfson, 2001).

Perez et al. (2000) also used the sacrificial-spacer approach for their synthesis of cholesterol-imprinted submicron beads. Carbonate ester was used as the sacrificial-spacer and the core-shell beads were prepared by two-step polymerisation. The first polymerisation step involved the emulsion polymerisation of methyl methacrylate or styrene monomers to produce an inner core-shell. The template cholesterol was then

covalently linked with the functional monomer to form chloresteryl (4-vinyl) phenyl carbonate (CVPC) which acted as the sacrificial-spacer. The second polymerisation step was then carried out with CVPC and ethylene glycol dimethacrylate (EGDMA) as the cross-linker. The template was removed using hydrolysis, which allowed the subsequent rebinding of cholesterol to the MIP via non-covalent interactions.

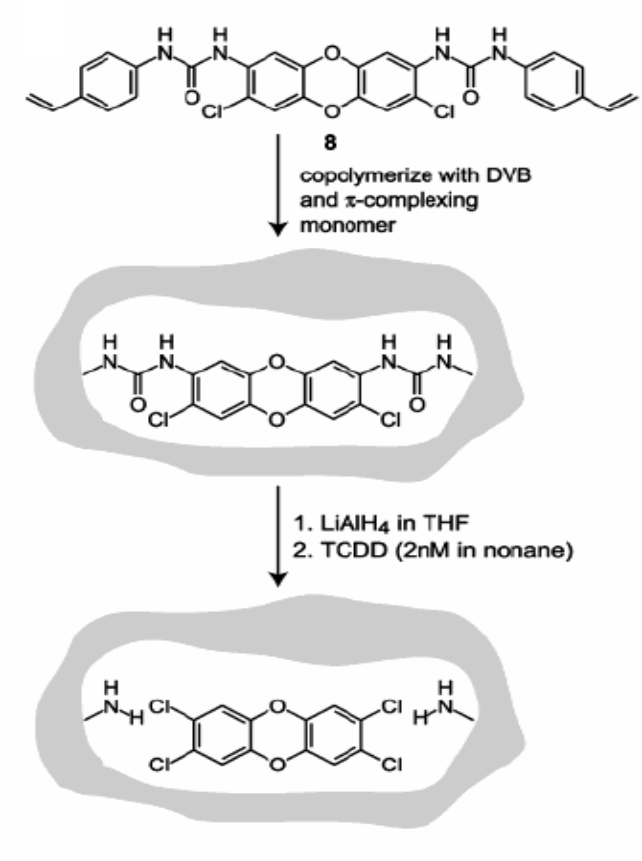

Figure 2.3 Imprinting 2,3,7,8-tetrachlorodibenzodioxin (TCDD) via the sacrificial-spacer approach (Whitcombe and Vulfson, 2001).

2.2.3 MIP beads

As mentioned earlier, one of the attractive properties of MIPs is that they can be prepared into various shapes and forms (beads, membranes, or films) suitable for the chosen application. In earlier preparations of MIPs, bulk polymerisation was used to produce monolithic imprinted polymers that were subsequently crushed, ground and sieved to the desired size. This conventional approach was not very efficient since it was time-consuming and produced irregular particles with a large size-distribution which are not favourable for applications like chromatography and solid-phase extraction (Mahony and Nolan, 2005; Kempe and Kempe, 2006). Bulk polymerisation is also unsuitable for scaling-up industrially due to the poor thermal dispersion during polymerisation. As a result, alternative methods of polymerisation have been proposed that would allow more control over the morphology of the imprinted particles, and which would also allow better heat dissipation during polymerisation.

There are many techniques to create MIPs with a uniform shape and size, and many researches focus on the synthesis and optimisation of MIPs in the spherical form such as beads and spheres. The desirable properties of these MIPs are: their uniform size with low polydispersity, their large specific surface area, and their potential to be applied at an industrial-scale. MIP beads and spheres, particularly in the micro- and nano-scales, are very suitable for the application of surface imprinting because of their large specific surface area available for the creation of binding sites. Another advantage is that the polymerisation involved in their synthesis, such as suspension (Mayes and Mosbach, 1996; Ansell and Mosbach, 1997; Flores et al., 2000), emulsion (Yoshida et al., 1999), or

miniemulsion (Vaihinger, 2002; Tan and Tong, 2007a), offers very good heat dissipation which enables them to be used on an industrial-scale. Further on in this literature review, we will discuss the application of MIP beads for protein surface imprinting.

2.3 Imprinting of proteins

Molecular imprinting is an effective technique to create artificial receptors which are able to specifically recognise target molecules. A large amount of literature could be found on the imprinting of small molecules, such as amino acids, drugs, and ions. The imprinting of macromolecules like proteins, however, is less common due to many inherent difficulties due to the larger and complex structure of the template molecules.

Proteins are large and complex biomacromolecules (generally with molecular weights of 10^3 to 10^4 Da) made up from amino acids which are linked together in a linear form by peptide bonds between the carboxyl and the amino group of adjacent residues. In the human body, proteins have a wide range of roles in all processes within the cell and many of them are enzymes which catalyse various biochemical reactions and are a key part of the metabolic system. Other proteins have mechanical and structural functions such as those which make up the cytoskeleton. Other vital roles in which proteins play an important part include: cell signalling, immune responses, cell adhesion, and the cell cycle.

Proteins fold into a specific conformation as a result of intramolecular non-covalent interactions, such as hydrogen and ionic bonding or van der Waals and hydrophobic forces.

To be able to perform their biological functions, proteins must conserve their folded three-dimensional structures, or their 'native' states. Taking an earlier example, enzymes are highly selective and only catalyse specific biochemical reactions in our body. This specificity is due to the shape of the enzyme molecules, held together by the intramolecular bonds which can be disrupted by changes in the surrounding conditions, such as the pH and temperature. This changes their shapes and as a result, the catalytic function of an enzyme is highly dependent on its environment.

The motivation behind protein imprinting is to imitate the ability of biomolecules, such as enzymes, to recognise molecules of a specific shape like a 'lock and key'. The current technology for the recognition of proteins for extraction, purification, and biosensing, greatly rely on binding assays of the target protein with antibodies. However, the disadvantages of this method include the high cost of these antibodies and their low stability which allows them to be used only under aqueous conditions. Another drawback which contributes to the high cost is that antibodies assays are only suitable for single use. MIPs, in contrast, are inexpensive, robust, and reusable, making them a suitable alternative to be used for selective protein binding (Turner et al., 2006; Ye and Mosbach, 2008).

2.3.1 Challenges in protein imprinting

There are many challenges associated with the imprinting of proteins compared to the imprinting of simpler and smaller molecules (Sellergren, 2000). The complex and flexible structure of proteins can lead to the non-homogeneity of the binding sites which would

result in low specificities of the MIPs (Bergmann and Peppas, 2008; Gai et al., 2008). In the pre-polymerisation mixture, a wide range of interactions between the monomers and various sections of the template protein are possible. This is due to the presence of numerous functional groups on the amino acids, which offers a large number of potential recognition sites over a relatively large surface area. Another difficulty is the incompatibility of the polymerisation conditions with the template protein, where the challenge is to conserve the native structure of the template so as to imprint the 'correct' conformation of the target protein. However, the difficulty lies in the fact that the structure of the protein can be easily modified and the protein can even be denatured due to the pH, temperature, ionic, or organic conditions of the polymerisation mixture, before or during polymerisation (Turner et al., 2006). In the synthesis of protein-imprinted polymers, one must study the structure of the protein throughout the entire process, especially making sure that the protein experiences no significant change in conformation during the polymerisation (Tan and Tong, 2007a).

Another problem linked to the incompatibility of the proteins with the polymerisation/imprinting environment is the fact that proteins are water-soluble compounds. Most imprinting systems rely on organic solvents in order to maximise the interaction, such as hydrogen bonding, between the functional monomer and the template molecule (Bossi et al., 2006; Janiak and Kofinas, 2007). The low solubility of proteins in non-polar solvents would limit the interaction between the functional monomer and the template as well as compromise their structure. Specific recognitions of biomolecules in the body, however, occur in an aqueous environment. The presence of water would greatly disrupt the formation of hydrogen bonds between the binding sites on the MIPs and the

protein. As a result, there is a need for MIPs which are able to be used for the recognition of proteins in an aqueous media.

Protein imprinting shares one drawback common to the imprinting of all macromolecules; MIPs suffer from unfavourable rebinding kinetics due to the slow diffusion of protein molecules to the binding sites. This problem is most severe in the conventional bulk imprinting method where the binding sites are located deep inside the polymer matrix. The low mass transfer of the large protein molecules through the matrix would render the rebinding kinetics unfavourable (Turner et al., 2006).

There are many successful methods adopted by various research groups to tackle the difficulties in protein imprinting. Surface imprinting and template immobilisation are two popular solutions and quite often these two techniques are employed together to optimise MIPs' specific recognition of proteins. They were first used for the targeting of smaller molecules but their usefulness was extended to the imprinting of macromolecules.

2.3.2 Surface imprinting

One of the major challenges faced in molecular imprinting, especially for the imprinting of macromolecules like proteins, is the ability for the target molecules to reach the binding sites of the MIP. In the conventional method of bulk imprinting, binding sites are produced within the 3D polymer matrix and as a result, the rebinding kinetics is often unfavourable due to steric hindrances, and limited diffusion and mass transfer. Another problem raised is the difficulty of template removal from the binding sites after

polymerisation. Inadequate washing of the newly formed MIP to remove the template would leave the binding sites 'occupied' and thus, rendering them unavailable to the target molecules for subsequent rebinding.

Surface imprinting is a popular technique to circumvent these problems and significantly improve the effectiveness of MIPs. In surface imprinting, binding sites are created on the surface of the MIP rather than in the interior of the polymer matrix, making them exposed and very accessible to the target molecules (Nicholls and Rosengren, 2001; Tan and Tong, 2007b). There are many approaches which have been investigated for the application of protein surface imprinting. Protein-imprinted film is one method with considerable success (Bossi et al. 2001; Piletsky et al., 2001; Ramanaviciene and Ramanavicius, 2004; Chou et al., 2005) but such MIPs are limited in their application and cannot be used in areas such as chromatography. MIP beads have been discussed earlier in this chapter (Section 2.2.3) and their numerous advantages, such as their large specific surface area, make them a suitable candidate for protein surface imprinting.

A classic example of MIP beads which were used for protein surface imprinting is the work by Kempe et al. (1995). Methacrylate groups were initially functionalised to the surface of silica beads and polymerisation was subsequently carried out in the presence of a metal chelating monomer, *N*-(4-vinyl)-benzyl iminodiacetic acid, copper ions, and RNase A as the template. The resulting MIP beads relied on metal coordination for the rebinding of RNase A and were used at the stationary phase in high-performance liquid chromatography (HPLC).

Hirayama et al. (2001) carried out the imprinting of lysozyme on surface-modified silica beads (0.025-0.040 mm) using a combination of acrylamide or *N*,*N*-dimethylaminopropylacrylamide with acrylic acid as the functional monomers. The resulting polymer pellet was then grounded and passed through a 0.15 mm sieve. In the rebinding tests, the two MIPs showed selectivity towards lysozyme over haemoglobin. Although the grinding of the pellet was required for the synthesis of the MIPs, Hirayama's work is not strictly a bulk imprinting approach due to the presence of the modified silica beads and the polymer layer which was formed on their surface.

Not only silica was utilised as the core particle for the synthesis of protein-imprinted beads but other supports, such as polystyrene, were also used. In the work by Yan et al. (2007), lysozyme and haemoglobin were successfully imprinted onto polystyrene microspheres. The styrene particles were first prepared by suspension polymerisation, after which the functional monomer, 3-aminophenylboronic acid, was grafted onto them in the presence of the template protein.

2.3.3 Template immobilisation

In the earlier discussion of the non-covalent approach to molecular imprinting, we have mentioned that despite of the favourable rebinding kinetics offered by this approach, one of its major drawbacks is the non-homogeneity of the binding sites. This is due to the relatively weaker interactions (non-covalent) between the functional monomers and the template molecules which cause less stable complexes to be formed in the pre-polymerisation mixture. This problem is exacerbated by the fact that proteins are complex

molecules which allow a wide range of interactions to take place with the functional monomers.

A popular solution to improve the homogeneity of the binding sites for the non-covalent imprinting of proteins is the immobilisation of the template molecule to a support before carrying out the polymerisation. There are many advantages of the template immobilisation approach. Templates which are insoluble in the polymerisation mixture and would not interact with the functional monomers could be imprinted since the immobilised protein molecules could be brought into contact with the functional monomers during polymerisation. Another advantage is that this approach prevents the aggregation of protein molecules which in turn would increase the homogeneity of the binding sites and increase the selectivity for their target molecule (Yilmaz et al., 2000; Bonini et al., 2007).

Shi et al. (1999) combined this approach with surface imprinting by immobilising various protein templates (albumin, immunoglobin G, lysozyme, ribonuclease and streptavidin) onto a mica surface. Disaccharide molecules were then used to coat the protein molecules, followed by the plasma deposition of hexafluoropropylene forming a 10–30 nm fluoropolymer thin film. After the removal of the mica and template protein, binding sites were left on the disaccharide layer which had the complementary shape of the template protein.

Silica beads were also used by Shiomi et al., 2005 as a support to covalently immobilise haemoglobin before surface imprinting was carried out with two kinds of organic silane

(3-aminopropyltrimethoxysilane and trimethoxypropylsilane) as functional monomers. Batch rebinding tests were carried out and the MIP beads prepared with template immobilisation exhibited higher binding specificity than their conventional non-immobilised template counterparts. The results seemed to indicate that template immobilisation has helped to produce binding sites which were more homogenous and possessed higher selectivity for the template protein.

Chapter 3

Optimising the preparation of protein surface-imprinted nanoparticles

3.1 Introduction

Molecular imprinting is an established technique to create biomics with specific recognition for the target molecule. Traditionally, it has been successfully applied to small molecules such as ions, amino acids, and small drugs. However, its application for macromolecules, like proteins, has been limited due to several inherent problems. Challenges in protein imprinting include: low rebinding kinetics, heterogeneity of binding sites due to the size and complexity of the protein molecule, incompatibility of the proteins with the solvents, and the entrapment of protein molecules in the polymer matrix.

As mentioned earlier in the introduction, Tan and Tong (2007a) had developed an effective technique to prepare RNase A surface-imprinted nanoparticles using miniemulsion polymerisation. In this part of the research, we aimed to optimise Tan's method and determine the factors and conditions which play an important part in determining the protein recognition efficiency. Bovine serum albumin (BSA) was used as the template protein rather than RNase A since it is cheaper and many batches of MIPs had to be synthesised.

3.2 Preparation of protein surface-imprinted nanoparticles via miniemulsion polymerisation

The following section is a detailed discussion of various aspects in the synthesis of RNase A surface-imprinted nanoparticles via miniemulsion polymerisation based on Tan's work.

3.2.1 Template: Ribonuclease A

RNase is a relatively small enzyme which catalyses the degradation of RNA into smaller components. RNase A is the main form of RNase found in the pancreas of *Bos Taurus* and consists of 124 amino acid residues (~13.7 kDa). Its sequence of amino acid residues was discovered in 1963 by Smyth et al., making it the first enzyme and the third protein whose sequence was correctly determined. Its chemistry, structure and functions have been extensively studied since its discovery and it has been widely used as the model system in various studies of proteins, enzymology, and molecular evolution (Carter and Ho, 1994).

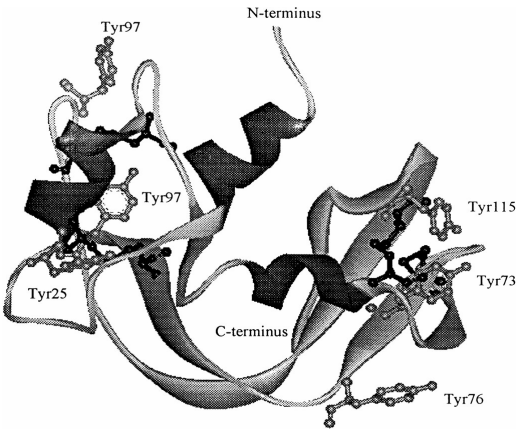

Figure 3.1 Ribbon diagram of RNase A showing the Tyr residues and the disulphide bonds (Stelea et al., 2001).

The stability of the template is an important factor which must be considered for successful imprinting. This is especially true for biomolecules such as proteins, since denaturation will cause a change in the structure of the template. The protein must be sufficiently stable to not unfold under the polymerisation conditions (Cormack and Elorza, 2004). In the work of Stelea et al. (2001), RNase A was shown to have significant denaturation between 50 ^{o}C and 70 ^{o}C in the presence of phosphate at neutral pH. Chen and Lord (1976) reported that a significant number of the alpha helices and the beta sheets remain in a solution of 0.1 M NaCl at 70 ^{o}C and pH 5.

3.2.2 Functional monomer: Methyl methacrylate

The choice of the functional monomer is of utmost importance and will directly affect the specificity of the MIPs. The monomer must be able to form a stable complex with the template so as to maximise the concentration of the complex in the polymerisation mixture. The rebinding environment for the intended application must also be kept in mind while

choosing the monomer. Biological systems are generally characterised by the dominating presence of water in the surrounding media and water molecules will significantly impair the ability of the target molecule to interact with the MIPs since they will compete to form hydrogen bonds with the binding sites (Ramstrom and Ansell, 1998).

Methyl methacrylate (MMA) is commonly used for miniemulsion polymerisation but not for protein imprinting. Methacrylic acid (MAA), however, is more popular as the functional monomer for non-covalent protein imprinting because the hydrogen atom of its carboxyl group can participate in hydrogen bonding with the template protein molecule. Very good separations have been achieved in non-aqueous environments where there were no water molecules to disrupt the interactions between the MAA and the amino acids of the target protein. However, it would be more beneficial if molecular recognition could be achieved in the presence of water since many applications for protein separation occur in the aqueous environment of biological systems. MMA was chosen because it is more hydrophobic than MAA and does not form hydrogen bonds in aqueous solutions. As a result, hydrophobic binding cavities are formed on the surface of the imprinted nanoparticles where hydrophobic interactions take place between the target protein and the shape-complementary binding sites in an aqueous environment.

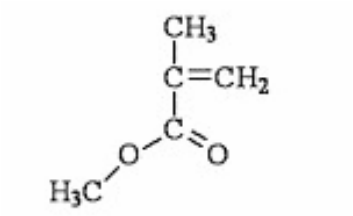

Figure 3.2 Structure of methyl methacrylate (MMA).

3.2.3 Cross-linker: Ethylene glycol dimethacrylate

Ethylene glycol dimethacrylate (EGDMA) is a common cross-linker and is often used for copolymerisation with MMA. The cross-linker plays three main roles: it controls the morphology of the MIPs, it holds the functional monomers in the positions complementary to the template and finally, it gives the imprinted polymer matrix mechanical strength. The cross-linker must be compatible with the imprinting system and must also be able to copolymerise with the functional monomer (Ramstrom and Ansell, 1998).

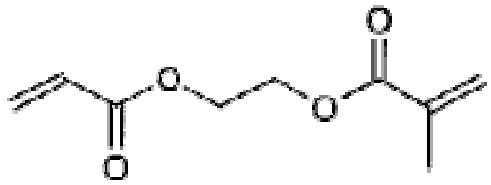

Figure 3.3 Structure of ethylene glycol dimethacrylate (EGDMA).

3.2.4 Miniemulsion polymerisation

Early preparations of MIPs relied on bulk polymerisation which produced monolithic imprinted polymers that were subsequently broken down and crushed. This was not a very effective method since it was time-consuming and produced irregular particles with a large size-distribution which were not favourable for applications like chromatography (Mahony et al., 2005). As a result, alternative methods of polymerisations have been proposed that allowed more control over the morphology of the imprinted particles.

Miniemulsion polymerisation is a method which produces regularly-sized spherical particles, typically in the range of 50-500 nm. This technique is similar to the conventional emulsion polymerisation but involves sub-micron oil-in-water dispersions, as well as the addition of a co-surfactant or co-stabiliser. In a typical set-up, the polymerisation mixture consists of water, monomer, co-stabiliser, and the surfactant and initiator systems (Asua, 2002). The important step in this method is the high-shear emulsification to produce sub-micron monomer droplets which are encapsulated by the surfactant micelles. This can be accomplished by devices such as a sonicator or homogeniser.

In Tan's method, sodium dodecyl sulphate (SDS) and poly (vinyl alcohol) (PVA) were used as the surfactant system in the miniemulsion. Despite the denaturing effects of the SDS, RNase A managed to retain its native conformation due to the presence of the PVA. Nagaranjan (2001) reported that non-ionic polymeric surfactants tend to interact with ionic surfactants micelles to form polymer-bound micelles. Sections of the polymer partially penetrate the polar surface of the micelles wrapping around them, and one polymer molecule could be associated with several surfactant micelles. As a result, this significantly decreases the critical micellar concentration (CMC) of the surfactant.

To start the polymerisation, Tan relied on redox initiation in order to minimise the denaturation of the protein. Sodium bisulphite and ammonium persulphate were used as co-initiators.

3.2.5 Factorial design

Factorial design is a common method used to design experiments which have several independent variables by examining simultaneously the effects of these variables (factors) and their interactions. It is an efficient method of investigation and is, therefore, widely used when then number of experiments that can be carried out is limited. For example: this can be due to the high cost associated with each run of the experiment or the amount of the time available is limited. In most factorial designs, each of the factors are studied at 2 levels, high (+) and low (-), and the experimental runs are carried out by varying these factors at all possible combinations. A total of 2^n experimental runs are performed, where n is the number of factors. In a half-fraction factorial design, only 2^{n-1} experimental runs are performed with the assumption that higher-order interactions are neglected, thus allowing the number of runs required to be halved (Kuehl, 1994; Mitchell, 2001).

In the preparation of the protein surface-imprinted nanoparticles via miniemulsion polymerisation, it is hypothesised that the imprinting efficiency of the resulting MIP is chiefly dependent on the following variables:

i) The ratio between the functional monomer and the cross-linker.
ii) The amount of template protein required.
iii) The polymerisation temperature.

Half-fraction factorial design was carried out with three independent variables (n = 3): functional monomer to cross-linker molar ratio (Factor A), amount of template protein

(Factor B), and polymerisation temperature (Factor C). As a result, MIPs and NIPs were synthesised under four different polymerisation conditions based on the half-fraction factorial design (Table 3.1a, b).

Treatment	A	B	C
T2	-	-	+
T3	+	-	-
T5	-	+	-
T8	+	+	+

Table 3.1a Half-fraction factorial design table with three factors (A, B, and C) and four treatments (T2, T3, T5, and T8). +/- represents the high and low levels, respectively.
A: MMA:EGDMA molar ratio
B: amount of BSA
C: polymerisation temperature

The table below shows the corresponding values of the high and low levels of each factor.

Factor	(+)	(-)
A) MMA:EGDMA	1 to 2.5	1 to 3.5
B) BSA (µmol)	1	0.5
C) Temperature (^{o}C)	45	40

Table 3.1b Values of the high and low levels (+/-) for the three factors.

3.3 Experimental section

3.3.1 Materials

Bovine serum albumin (BSA), methyl methacrylate (MMA, 99%), ethylene glycol dimethacrylate (EGDMA, 98%), sodium dodecyl sulphate (SDS, minimum 98.5% GC),

sodium bicarbonate (99.7-100.3%), sodium bisulphite (minimum 99%), ammonium persulphate (98%), and trifluoroacetic acid (TFA, 99%) were purchase from Sigma-Aldrich (USA). Poly (vinyl alcohol) (PVA, 80 mol% hydrolyzed, MW 6000) and ethanol (absolute grade for analysis) were purchased from Polysciences, Inc. and Merck (Germany), respectively. Acetonitrile (HPLC grade) and acetic acid (Glacial) were purchased from FisherChemicals (USA). The chemicals were used as is without further purification.

3.3.2 Preparation of BSA-imprinted nanoparticles

The experimental protocol for the synthesis of the MIPs was modified from the work of Tan and Tong (2007a). The experiment was scaled down by a factor of two (i.e. the amount of the reactants was halved), allowing a simpler experimental setup and therefore, many batches of MIPs were prepared in a shorter time. The amount of chemicals and conditions used for the four batches of MIPs is stated in the following tables.

Treatment	Temperature (^{o}C)	EGDMA (µl)	MMA (µl)	BSA (mg)
T2	45	2100	339.88	34.38
T3	40	2100	475.84	34.38
T5	40	2100	339.88	68.75
T8	45	2100	475.84	68.75

Table 3.2a Variations of the three factors across the four treatments.

PVA (g)	SDS (mg)	Sodium Bicarbonate (mg)	DI Water (ml)
0.1875	28.85	23.45	10

Table 3.2b Composition of the first aqueous phase.

PVA (g)	SDS (mg)	DI Water (ml)
0.0400	40.00	80

Table 3.2c Composition of the second aqueous phase.

Sodium bisulphite (g)	Ammonium persulphate (g)
0.115	0.126

Table 3.2d Amount of initiators.

The first aqueous phase was prepared by dissolving PVA, SDS and sodium bicarbonate in 10 ml of deionised (DI) water. The second aqueous phase was prepared by dissolving only PVA and SDS in 80 ml of DI water. The functional monomer and cross-linker, MMA and EGDMA, were added to the first aqueous phase and the mixture was sonicated (Sonics Vibracell VCX 130) at 70% amplitude for 60 seconds to obtain a miniemulsion. The template protein, BSA, dissolved in 800 μl of DI water, was added to the miniemulsion and stirred magnetically for 30 minutes to allow sufficient template-monomer interactions. The miniemulsion was then added drop-wise to the second aqueous phase while stirring. The reaction mixture was pre-purged for 15 minutes with nitrogen gas and each of the initiators, sodium bisulphite and ammonium persulphate, were dissolved in 1500 μl of DI water before being injected to the reaction mixture. Polymerisation was carried-out for 24 hours at the specified temperature, with mechanical stirring at 300 rpm (RW20, Ika Labortechnik, Germany).

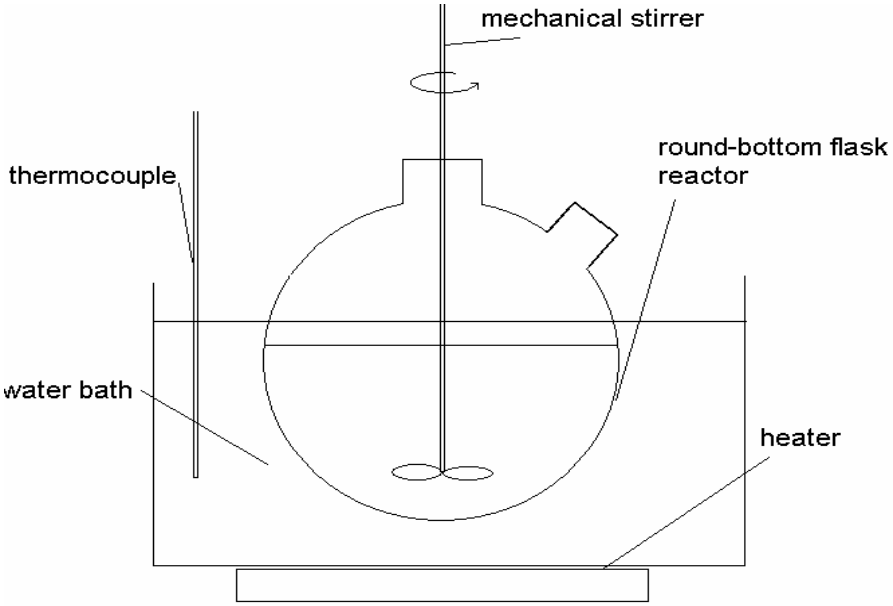

Figure 3.4 Polymerisation reactor setup.

The resulting MIP solution was then washed 5 times with DI water, and 5 times with SDS:Acetic acid solution (10 w/v%:10 v/v%) to remove the template protein. Finally, it was washed 4 times with ethanol and 6 times further with DI water to remove the remaining surfactant and any unreacted monomers. For each washing, the polymer solution was centrifuged at 9000 rpm for 60 minutes (Universal 32R, Hettich Zentrifugen, Germany). The final MIP was stored in DI water.

3.3.3 Preparation of non-imprinted nanoparticles

The preparation was identical except for the addition of the protein and the NIPs were washed in the similar manner with DI water, SDS:Acetic acid solution (10 w/v%:10 v/v%), and ethanol.

3.3.4 Batch rebinding tests

To study the specificity of the MIPs, batch rebinding test with 1.8 mg/ml BSA solution was carried out. The same test was repeated with NIPs as a control.

A stock BSA protein solution of 4 mg/ml was prepared. 1 ml was drawn from it and added to 1 ml of DI water to obtain the first standard solution of 2.0 mg/ml. DI water was then added to the stock solution to decrease its concentration to 3.6 mg/ml. Another 1 ml was drawn and added to 1 ml of DI water, like before, to obtain the second standard solution of 1.8 mg/ml. For the batch rebinding, 2 ml of the 3.6 mg/ml stock solution was drawn and added to 2 ml of the well-mixed polymer solution. This was repeated two more times to obtain three tubes of rebinding mixture. The third and fourth standard solutions of 1.6 and 1.4 mg/ml respectively were prepared in the similar manner. This method of preparation was designed to minimise the systematic and random errors in the preparation of the standard protein solutions for the plotting of the calibration curve.

Concentration of stock solution (mg/ml)	Volume of stock solution (ml)	Volume remaining after 1 ml protein solution is drawn (ml)	DI Water added to stock solution (ml)
4.0	15.00	14.00	1.556
3.6	15.56	8.56*	1.069
3.2	9.63	8.63	1.232
2.8	9.86	8.86	

*Table 3.3 Preparation of the stock solution for the batch rebinding test of one set of MIP. *A total of 7 ml of stock solution of 3.6 mg/ml was drawn (1 ml for the standard solution and 3x2 ml for the batch rebinding).*

The rebinding mixtures were then mixed using a Rotamix (RKVS, ATR Inc., Japan) and after 24 hours, it was centrifuged at 9000 rpm for 60 minutes. The supernatant was withdrawn with a syringe and then filtered through a 0.2 μm filter unit into an HPLC valve. The four standard solutions were also filtered similarly and their protein concentrations were determined via HPLC analysis.

A reversed-phase column (Agilent Zorbax 300SB-C18, 4.6 x 150 mm, 5 μm, USA) was used on an Agilent 1100 series (USA) HPLC system. Two solvents were used for the mobile phase; A: 0.1% trifluoroacetic acid (TFA) and 100% water, and B: 0.09% TFA, 80% acetonitrile, and 20% water. The UV detector was set at 220 nm absorbance and the injection volume was 50 μl. The mobile phase flow rate was 1 ml/min and solvent B was changed from 25% to 70% in 40 minutes in order to create a linear gradient elution.

The loading (amount of BSA adsorbed per amount of polymer) of the MIPs and NIPs is calculated using the formula below:

$$Q = \frac{[C_I - C_F] \times 4\ ml}{m}$$

Q : Amount of adsorbed BSA (mg) / amount of polymer (g)

C_I : Initial BSA concentration (mg/ml)

C_F : Final BSA concentration (mg/ml)

m : Mass of polymer in 2 ml of polymer solution (g)

The amount of MIP present in 2 ml of polymer solution was determined by adding 2 ml of the well-mixed polymer solution to a 2 ml Eppendorf tube. The tube was then freeze-dried for 24 hours and weighed. The difference between this mass and the mass of the empty Eppendorf tube gave the amount of MIP present. This was repeated five times and the average mass was taken.

3.3.5 Determination of the swelling ratio

2 ml of well-mixed polymer solution was added to a 2 ml Eppendorf tube and was centrifuged at 9000 rpm for 60 minutes. The supernatant was pipetted out and the tube was weighed to obtain the swollen weight of the particles (W_{wet}). The tube was then freeze-dried for 24 hours and weighed to obtain the dry weight of the particles (W_{dry}). The swelling ratio (SR) was calculated from the following equation:

$$SR = \frac{W_{wet} - W_{dry}}{W_{dry}}$$

3.3.6 Determination of the particle size using field-emission scanning microscope

The particles were observed under FESEM (JSM-6700F, JEOL, USA) with platinum coating and a total of a hundred particles from two different areas were measured to determine their average diameter.

3.4 Results and discussion

3.4.1 Size and morphology of the MIPs and NIPs

The FESEM images (Figure 3.5A, B) show that nanoparticles were successfully synthesised in the miniemulsion polymerisation. The particles were spherical, highly uniform and monodispersed with diameters ranging from 40 nm to 50 nm under the different treatments (Figure 3.6). These particles were therefore suitable for the imprinting of large macromolecules like proteins since they had a large surface area available for the creation of binding sites which are easily accessible to the target molecules. The particles were also suitable for applications in chromatography due to their monodispersity and uniformness.

The diameters of the nanoparticles obtained in this work were slightly larger than those reported in the work of Tan and Tong (MIP: 37.6 nm $\pm$ 5.3, NIP: 41.0 nm $\pm$ 6.4). This may be due to the difference in the method used to form the miniemulsion. In this work, a sonicator was used rather than a homogeniser, which was used in Tan's work. Another possible cause is the difference in the volumic ratio between the first and second aqueous phases; 1:8 compared to 1:20 from Tan's work. This might have affected both the stability of the miniemulsion and subsequently, the size of the particles.

(A)

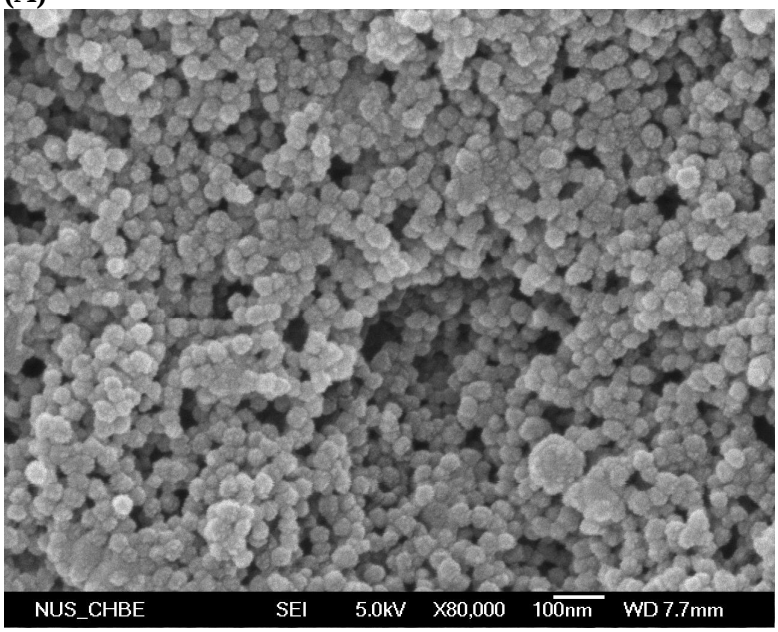

(B)

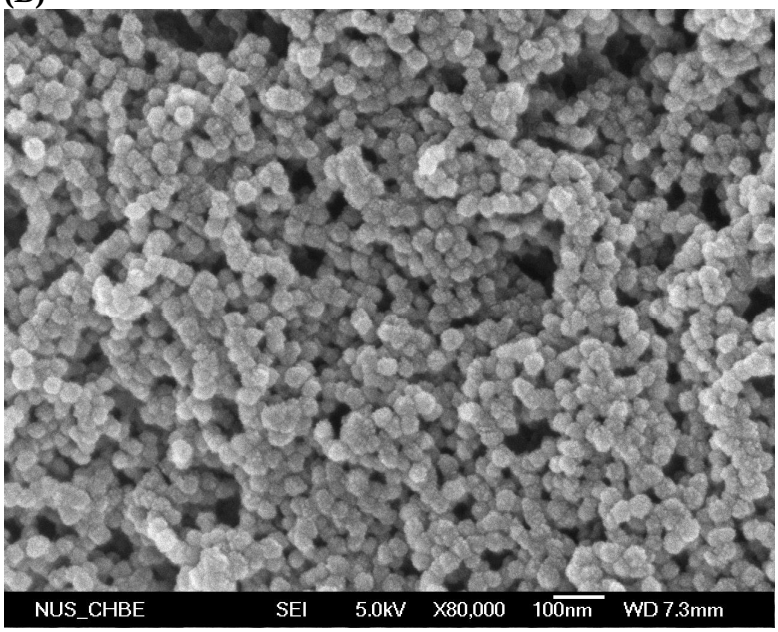

Figure 3.5 FESEM images of: (A) MIPs and (B) NIPs under treatment T2.

There were no significant differences between the size and morphology of the MIPs and the NIPs (Figure 3.5A, B). This would mean that any difference in the BSA loading during the batch rebinding tests of the MIPs and NIPs cannot be contributed to the

difference in particle size and morphology. There was also no significant trend in the particle diameters under the different treatments.

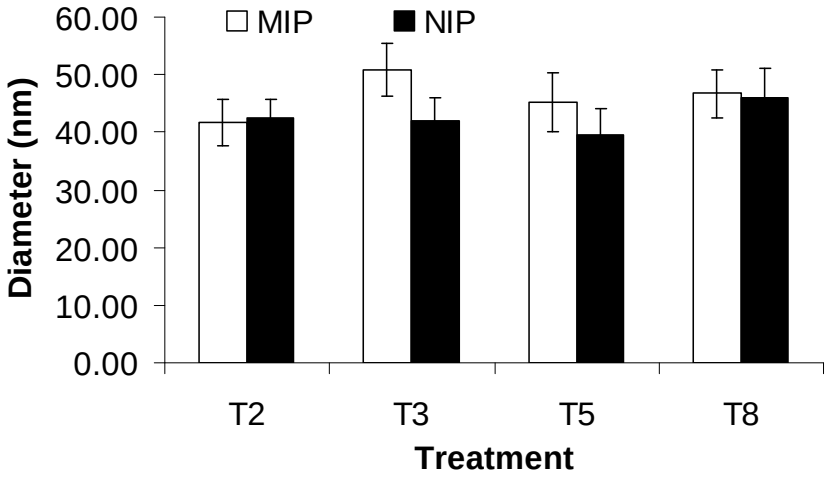

Figure 3.6 Diameter of the nanoparticles from the four treatments.

The swelling ratios (SR) of the MIPs and NIPs varied between 20 and 45 (Figure 3.7). No significant trend was observed but the NIPs on all the treatments seemed to have a higher SR on average than the MIPs (treatment T5 in particular). This was unexpected because the MIPs and NIPs were synthesised in the same way except for the addition of the protein. This discrepancy was most likely due to the following experimental errors:

i) The microbalance was very old and did not give consistent readings. Significant variations were observed in spite of repeated weighing.

ii) The pipetting of the supernatant to leave behind the wet polymer after centrifuging was probably the biggest cause of error. It was very difficult to pipette the supernatant and not draw up any particles. If particles were drawn up with the supernatant, the mass of the swollen and dry polymer (W_{wet} and

W_{dry} respectively) would have been smaller than the true value. This problem can be avoided by not pipetting all of the supernatant but the W_{Wet} would be higher than the true value. Decanting was not effective despite centrifuging at 10000 RPM for 60 minutes.

iii) The inaccuracy in obtaining the W_{Wet} was further amplified due to the fact that the total mass of the Eppendorf tube and the particles was small. The percentage error was quite large because of the relatively small samples being measured. In Tan's work, 5 ml of polymer solution was added to 15 ml centrifugal tubes. As a result, the resulting percentage error due to the above problem was smaller.

Polymer swelling plays an important role in the performance of the MIPs and therefore, it is beneficial to study the SR of the MIPs (Piletsky et al., 2004). The SR shows the extent of cross-linking within the particle; the smaller the SR, the greater level of cross-linking achieved during polymerisation. Thus it indicates how firmly the functional monomers are held in the 3D matrix (Lu et al., 2006). This is important since the selectivity of the MIPs depends on how well the orientations of the functional monomers in the binding sites are preserved after the template is removed. However, small adjustments may be advantageous since it may help accommodate the large flexible protein molecule when it binds to the imprinted sites (Sellergren, 2001). The SR values obtained in this work were much higher than those obtained in Tan's work (~4-7). It is possible that the cross-linking during the polymerisation was not extensive but the high SR values observed might have been caused by the errors mentioned earlier.

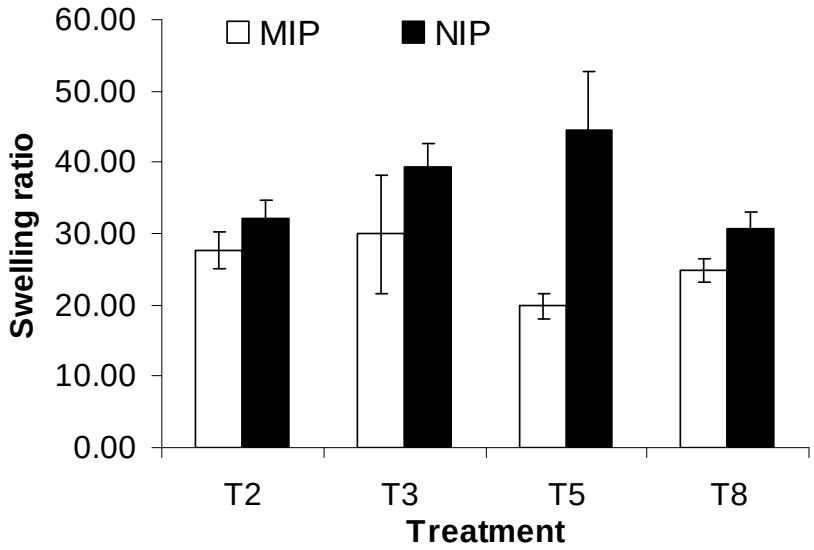

Figure 3.7 Swelling ratios of the nanoparticles from the four treatments.

3.4.2 Batch rebinding tests

Batch rebinding tests of the MIPs and NIPs were carried out with 1.8 mg/ml BSA protein solution. Figure 3.8 shows the protein loading of the nanoparticles prepared under the 4 treatments.

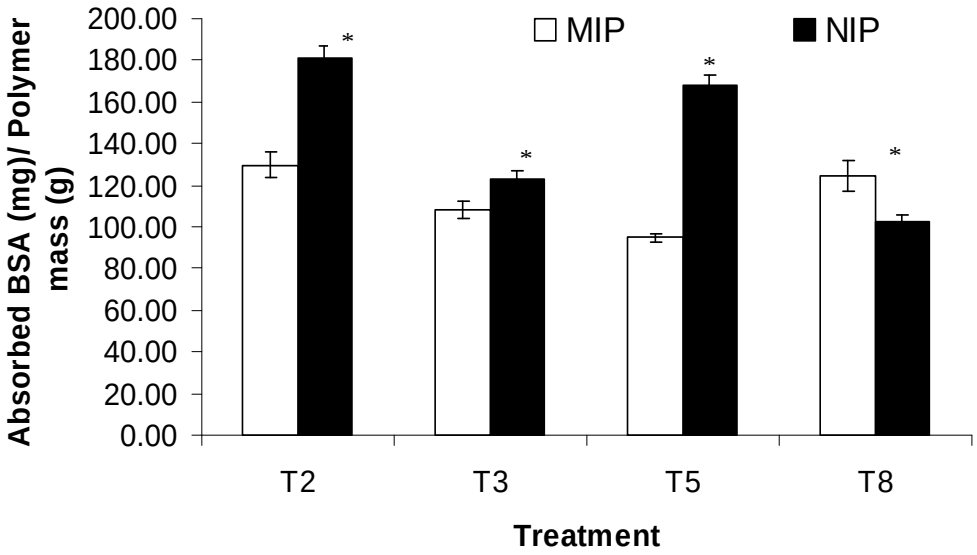

*Figure 3.8 Batch rebinding tests of BSA for MIP and NIP of the 4 treatments. Student's t-test, *: $p < 0.05$.*

The loading for the NIPs was significantly higher than that of the MIPs for treatments T2, T3, and T5. This was unexpected since the MIPs were supposed to show preferential binding towards BSA which was the template molecule, and the NIPs were expected to display only a limited loading due to non-specific adsorptions. Therefore, specific adsorption was not achieved and imprinting was unsuccessful in the above treatments. The NIPs loadings were in the range of 100 to 180 mg BSA/ g polymer which were much higher than the value of 55 mg/g reported in Tan's work for an initial BSA concentration of 1.6 mg/ml. Higher loading will be observed for higher initial BSA concentration of the rebinding protein solution but this was insufficient to explain the much greater loading observed when the initial BSA concentration was 1.8 mg/ml. The difference could not also be explained by looking at the particle size since the NIPs in Tan's work were similar in size (41.0 nm) to the ones in this work (42.6 nm).

Only treatment T8 showed preferential binding towards BSA with MIPs loading of 124.55 mg/g and NIPs loading of 102.28 mg/g. The relative loading (MIPs loading / NIPs loading) for treatment T8 is equal to 1.22. Treatment T8 corresponds to the condition where all the 3 factors are in their 'high' state:

a) MMA:EGDMA ratio = 1:2.5

b) Amount of BSA added to the pre-polymerisation miniemulsion = 1 µmol

c) Polymerisation temperature = 45 ^{o}C

In the work of Fish et al. (2005), it was proposed that increasing the number of the functional monomers and template will maximise the interactions between the two species and yield more selective binding sites on the MIP. However, the use of excessive functional monomers will encourage the formation of non-specific sites. An optimal functional monomer-template ratio is achieved when a balance is reached in the monomer-template equilibrium during the polymerisation. In this experiment, the increased number of MMA present may have improved the extent of template-functional monomer complex formation. As a result, the number of binding sites formed on the surface of the nanoparticles was increased and therefore, leading to a higher specific BSA adsorption. Increasing the amount of BSA during the imprinting step would also have a similar effect of increasing the template-functional monomer complex formation.

The increase in temperature may have improved the extent of polymerisation and cross-linking. However, raising the temperature to an excessive level would cause the protein to lose its native structure. BSA is a very stable protein which could withstand high

temperatures before denaturing and it was reported by Poole et al. (1987) that BSA experiences negligible conformational changes at temperatures below 58.1 ^{o}C.

The loading for the MIPs prepared with treatment T8 was much smaller than the value reported in Tan's work. The ribonuclease A (RNase A)- imprinted nanoparticles prepared by Tan achieved a maximum loading of 744.9 RNase A mg/ polymer g (~54.3 RNase A μmol/ polymer g) whereas our BSA-imprinted nanoparticles had a loading of 125 BSA mg/ polymer g (1.52 BSA μmol/ polymer g). Care must be taken while comparing the two values since the MIPs were synthesised differently and the template protein was different. RNase A is a smaller protein with only 124 amino acid residues whereas BSA has 583 residues and so we would expect the nanoparticles to adsorb and accommodate large molecules less readily than smaller ones. However, this alone will not be sufficient to explain the dramatic decrease in the protein loading.

As mentioned earlier, the swelling ratio is a direct indication of the cross-linking and how well the orientations of the functional monomers are preserved in the imprinted sites. The large SRs of the nanoparticles in treatments T2, T3, and T5 might have explained why preferential binding was not achieved, and only treatment T8 showed a significant selectivity for the target protein. On average, treatment T8 produced nanoparticles (MIPs and NIPs) with the smallest SR of 27.8 whereas the SRs for T2, T3, and T5 are 29.9, 34.7, and 32.2, respectively. Furthermore, the SRs of the nanoparticles synthesised with this modified protocol are nearly 10 times larger than the values reported in Tan's work, indicating that the modified protocol produced MIPs which were not cross-linked extensively. Molecular imprinting relies on shape-complementary binding sites in order to

selectively bind to the target molecule and thus, MIPs possessing binding-sites which are not well-defined and well-preserved would display limited or no specific recognition.

3.5 Conclusion

3.5.1 Summary

In this work, using a modified protocol based on Tan's work, BSA surface-imprinted nanoparticles were synthesised by the redox-initiated miniemulsion polymerisation of MMA and EGDMA. The resulting particles were monodispersed uniform spheres with diameters ranging from 40 nm to 50 nm. Four different sets of MIPs and NIPs were prepared under conditions which were varied according to a three-factor half-fraction factorial design. The three factors were: the MMA:EGDMA molar ratio, the amount of BSA used for imprinting, and the polymerisation temperature. The MIPs in the first three treatments did not display any recognition property in the aqueous rebinding tests but molecular recognition was exhibited in the last treatment (treatment T8) when all the factors were in the 'high' state. Factorial data was not able to be generated and analysed because only one treatment showed measurable specific recognition for the BSA. As a result, the factorial design optimisation analysis could not be completed.

One plausible explanation for the MIPs' failure to exhibit any preferable uptake of the BSA is that their swellings ratios were nearly 10 times higher than the values in Tan's work. On the other hand, MIPs from treatment T8 had the lowest SR and were able to

specifically recognise the protein. The high polymerisation temperature had increased the extent of reaction and the amount of cross-linking, which preserved the shape-complementary binding sites on the surface of the nanoparticles. Furthermore, the high MMA:EGDMA ratio and the large amount of protein had aided the formation of protein-monomer complexes, promoting the creation of specific binding sites. As a result, all of the 3 factors played an important role in this protein surface imprinting technique.

3.5.2 Recommendations

i) Several batches could be synthesised in order to confirm the batch-to-batch reproducibility of results.

ii) The batch rebinding tests should be carried out for a range of BSA concentrations in order to study the dependence of the imprinting efficiency on the protein concentration.

iii) The surface areas of the MIPs and NIPs prepared by the four treatments should be determined in order to study their effects on the imprinting efficiency.

iv) This work was carried out with the assumption that Tan's protocol could be successfully applied to an alternate template protein, BSA, rather than RNase A, which was the original protein used. An additional control must be performed which involves the synthesis of BSA-imprinted nanoparticles using the original protocol to verify whether molecular imprinting can be achieved with Tan's method when BSA is used as the template protein.

Chapter 4

Investigating protein-surfactant interactions in the preparation of protein surface-imprinted nanoparticles

4.1 Introduction

In the previous chapter, we looked at bovine serum albumin (BSA) surface-imprinted nanoparticles prepared via miniemulsion based on Tan's protocol (Tan and Tong, 2007a). In order to determine the principle factors which affect the imprinting efficiency, an optimisation analysis was carried out. Below are the three variables which were chosen:

i) The ratio between the functional monomer (MMA) and the cross-linker (EGDMA).
ii) The amount of template protein (BSA) required.
iii) The polymerisation temperature.

The optimisation analysis was not complete because out of the four sets of treatment conditions, only one condition resulted in BSA-imprinted particles which displayed significant molecular recognition.

Following the recommendations of the previous study, a follow-up investigation was carried out to determine whether molecular recognition could be achieved with an alternative template protein using the unmodified protocol from Tan's work for the

synthesis of ribonuclease A-imprinted nanoparticles. The chosen template protein was bovine serum albumin (BSA) which was the protein used in the previous chapter. Lysozyme (Lys) was also used as an alternative protein because it is similar in size to the original template protein, ribonuclease A (RNase A). The morphological features (size, surface area, and swelling ratio) of the nanoparticles were characterised and various batch rebinding tests were carried out to compare the relative imprinting efficiencies of the imprinted particles using the three template proteins. Furthermore, circular dichroism (CD) spectropolarimetry was employed to study the relative interactions of the three template proteins and the surfactant in the miniemulsion polymerisation system in order to gain a deeper understanding of the mechanisms involved during the imprinting process.

4.2 Experimental section

4.2.1 Materials

The same materials were used as the previous chapter. The Lys from chicken egg white and RNase A from bovine pancreas were purchased from Sigma (USA).

4.2.2 Preparation of RNase A-, BSA- and Lys-imprinted and non-imprinted nanoparticles

The protocol to synthesise RNase A-, BSA- and Lys-imprinted nanoparticles (RMIP, BMIP, and LMIP) was directly taken from Tan's work (Tan and Tong, 2007a). The

procedure was similar to the one used in the previous chapter but different amount of chemicals were used and the polymerisation was carried out at 40 degrees Celsius. To synthesise the imprinted nanoparticles, 1.87 μmol of the template protein was added. Table 4.1 summarises the amount of chemicals used.

Temperature (^{o}C)	EGDMA (ml)	MMA (ml)	RNase A (mg)	BSA (mg)	Lys (mg)
40	4.2	0.8	25.6	123.2	27.4

Table 4.1a Composition of the oil phase.

PVA (g)	SDS (mg)	Sodium Bicarbonate (mg)	DI Water (ml)
0.375	57.7	46.9	20

Table 4.1b Composition of the first aqueous phase.

PVA (g)	SDS (mg)	DI Water (ml)
0.2	200	400

Table 4.1c Composition of the second aqueous phase.

Sodium bisulphite (g)	Ammonium persulphate (g)
0.23	0.252

Table 4.1d Amount of initiators.

The washing steps were identical to the previous chapter. As before, the non-imprinted particles (NIPs) were synthesised in the same way as the MIPs except for the addition of the template protein.

4.2.3 Elemental analysis

To demonstrate the complete removal of the template protein from the imprinted polymer after the extensive washing, elemental analysis (CHNS/O Analyzer Series II 2400, Perkin Elmer, USA) was carried out on Ribonuclease A-imprinted nanoparticles.

4.2.4 Determination of morphological features

The sizes of the particles were determined, as before, by direct observation under the FESEM. Specific surface area was measured using the nitrogen sorption method (NOVA 3000 series, Quantachrome Instruments, USA) and 7-point Brunauer-Emmett-Teller (BET) calculation. The swelling ratio (SR) of the MIPs and NIPs were calculated from the equation below where W_{wet} and W_{dry} are the wet and dry polymer mass, respectively.

$$SR = \frac{W_{wet} - W_{dry}}{W_{dry}}$$

4.2.5 Batch rebinding tests

The batch rebinding tests were carried out on the MIPs and NIPs in a similar method to the previous chapter but on a larger scale. 5 ml of the imprinted polymer solution was added to 15 ml centrifuge tubes followed by 5 ml of stock protein solution of different concentrations to make up rebinding mixtures of 10 ml at various protein concentrations (0.8, 1.0, 1.2, 1.4, 1.6 mg/ml). Six tubes were prepared for each final protein concentration.

The same procedure was repeated for the NIPs. As in the previous chapter, the tubes were then mixed for 24 hours and centrifuged. The final protein concentration was analysed using a HPLC, as before, in order to determine the protein loading of the polymer using the equation below:

$$Q = \frac{[C_I - C_F] \times 10\ ml}{m}$$

Q : Amount of adsorbed protein(mg) / amount of polymer (g)

C_I : Initial protein concentration (mg/ml)

C_F : Final protein concentration (mg/ml)

m : Mass of polymer in 5 ml of polymer solution (g)

To determine m, an empty 15 ml centrifuge tube was weighed and 5 ml of well-mixed polymer solution was added to the tube. The solution was then freeze-dried and the tube was weighed again to obtain the weight difference.

4.2.6 Competitive batch rebinding tests

The selectivity of the MIPs and the NIPs were further investigated in competitive rebinding tests where the rebinding solution contained more than one type of protein. In the binary batch rebinding test, 5 ml Ribonuclease A polymer latex (RMIP) were added into 15 ml centrifuge tubes and a rebinding protein solution containing both RNase A and BSA were added in order to achieve an initial protein concentration in the tube of 1.2

mg/ml for each protein. The rebinding was then carried out as before and the final protein concentration was then measured. This was repeated for the NIPs. The following parameters were then calculated in order to characterise the selectivity of the RMIPs:

$$K_D = \frac{C_p}{C_s}$$

K_D : Static distribution coefficient (ml/g)

C_p : Amount of ligand adsorbed (μmol/g)

C_s : Free ligand concentration (μmol/ml)

$$\alpha = \frac{K_{D1}}{K_{D2}}$$

α : Separation factor

K_{D1} : Static distribution coefficient of template molecule (ml/g)

K_{D2} : Static distribution coefficient of control molecule (ml/g)

$$\beta = \frac{\alpha_1}{\alpha_2}$$

β : Relative separation factor

α_1 : Separation factor of MIP

α_2 : Separation factor of NIP

The ternary rebinding test was carried out in a similar manner for the four batches of polymer synthesised; NIP, RMIP, BMIP, and LMIP. The rebinding protein solution

containing RNase A, BSA, and Lys was added to the 5 ml polymer latex in a 15 ml tube in order to achieve an initial protein concentration in the tube of 1.8 mg/ml for each of the protein. All of the rebinding tests were done in triplicates.

4.2.7 Kinetics study

The adsorption kinetics of the RMIP and NIP were studied as follow. 5 ml RMIP solution was added into a 15 ml centrifuge tube followed by 5 ml of RNase A solution, giving an initial protein solution of 1.8 mg/ml in the tube. The tube was then attached to a rotamix and adsorption was carried out under room temperature and 1 ml sample was drawn at various intervals and sent to the HPLC to determine its protein content.

4.2.8 Desorption study

In a 15 ml centrifuge tube, 5 ml RMIP solution was added to 5 ml of RNase A solution, giving an initial protein solution of 1.8 mg/ml. Adsorption was allowed to take place under room temperature for 24 hours after which the amount of RNase A adsorbed was analysed like before. The protein-loaded RMIP was then isolated after 1 hour of centrifugation at 9000 rpm and redispersed in 2 different types of solvent, pure water and acetonitrile/water (1:1). Desorption was carried out for 24 hours on a Rotamix and the concentration of the desorbed protein was determined with a HPLC.

4.2.9 CD study

The interactions between the surfactant in the miniemulsion polymerisation mixture and the 3 proteins were investigated using CD spectropolarimetry. Protein was added to a surfactant solution of SDS (10 mM) and to another consisting of SDS (10 mM)/PVA (1.5% w/v). The samples were analysed in a 5-mm round cuvette using the CD spectropolarimeter (JASCO J-810, UK) with continuous mode, at a scan speed of 50 nm/min and wavelength ranging from 180 nm to 300 nm.

4.3 Results and discussion

4.3.1 Size and morphology of the MIPs and NIPs

The miniemulsion polymerisation reaction was successful in synthesising nanoparticles which were uniform, spherical, and highly monodispersed. From the FESEM images (Figure 4.1), there was not any noticeable difference in morphology between the 4 sets of polymer and the diameter was approximately 40 nm, comparable to those in the previous chapter.

The swelling ratio (SR) reflects directly the extent of cross-linking in the polymer matrix and how well the functional monomers conserve their orientations in the binding sites (Lu et al., 2006). The SR of the particles ranged from 3-5 which were similar to those shown in the work of Lu et al. (2006) and were much smaller than the ones in the previous

chapter (~30). This showed that the imprinted and non-imprinted polymers were cross-linked effectively.

There was not any significant difference in the specific surface areas of NIP, RMIP, and LMIP (~26 m^2/kg) calculated from the nitrogen sorption BET analysis. On the other hand, the value for the BMIP was much lower at 14 m^2/kg which was unexpected because the polymers were all synthesised in the same way. The exact reason for this difference is not known but it is hypothesised that it was due to the difference in interaction between the protein and the monomer during the polymerisation which will be explained further in detail in Section 4.3.7. The surface areas obtained in this work were much smaller than those synthesised by Vaihinger et al. (2002) (~58.0 m^2/kg), despite the fact that our particles were approximately 5 times smaller. This may have been due to the fact that the nanoparticles in Vaihinger's work were much more porous and the presence of the pores would have greatly increased the specific surface area. Our particles, however, did not appear to have pores from the FESEM images. Furthermore, they were lyophilised before the nitrogen sorption measurement was carried out and this would have caused extensive agglomeration, resulting in a much lower apparent specific surface area. Large surface area on the imprinted polymer is beneficial because more binding sites could then be situated on the surface of the polymer matrix, and thus improving the adsorption and desorption kinetics. However, having a surface area which is too large may be detrimental due to the larger non-imprinted area available for non-specific loading.

(A)

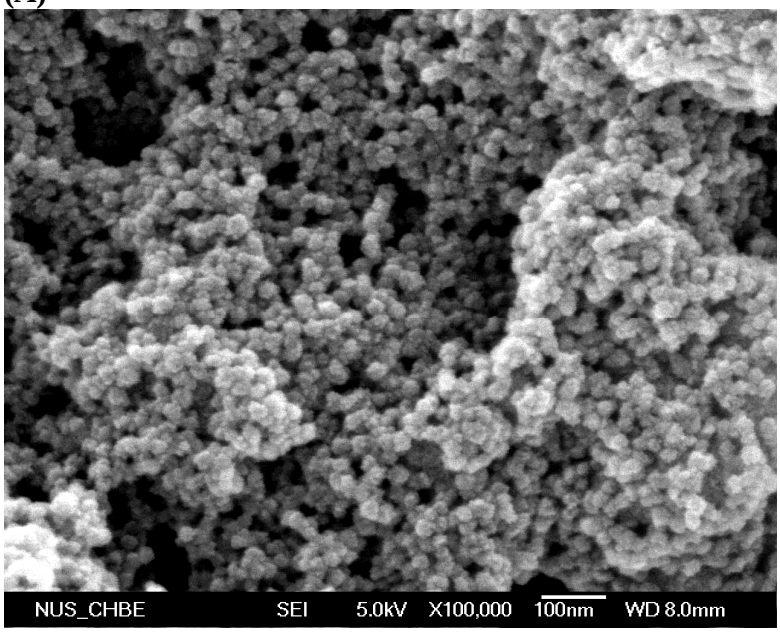
NUS_CHBE SEI 5.0kV X100,000 100nm WD 8.0mm

(B)

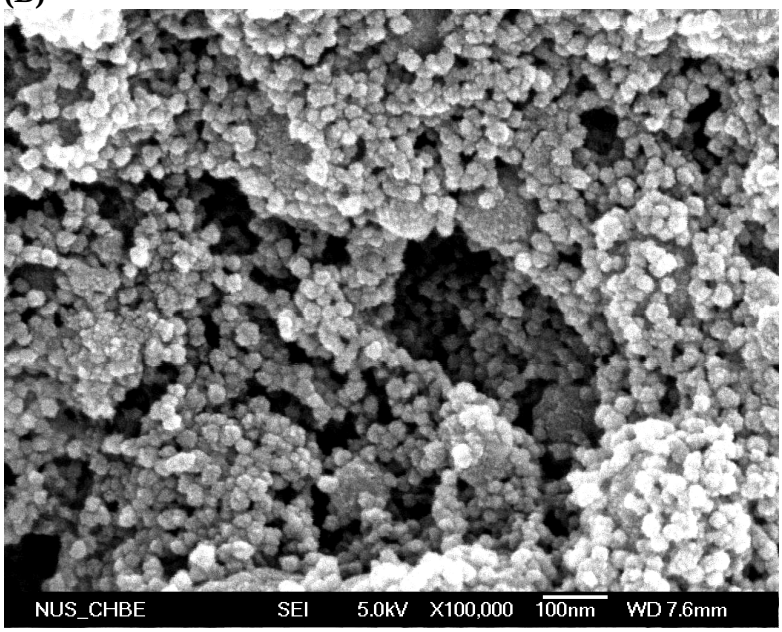
NUS_CHBE SEI 5.0kV X100,000 100nm WD 7.6mm

(C)

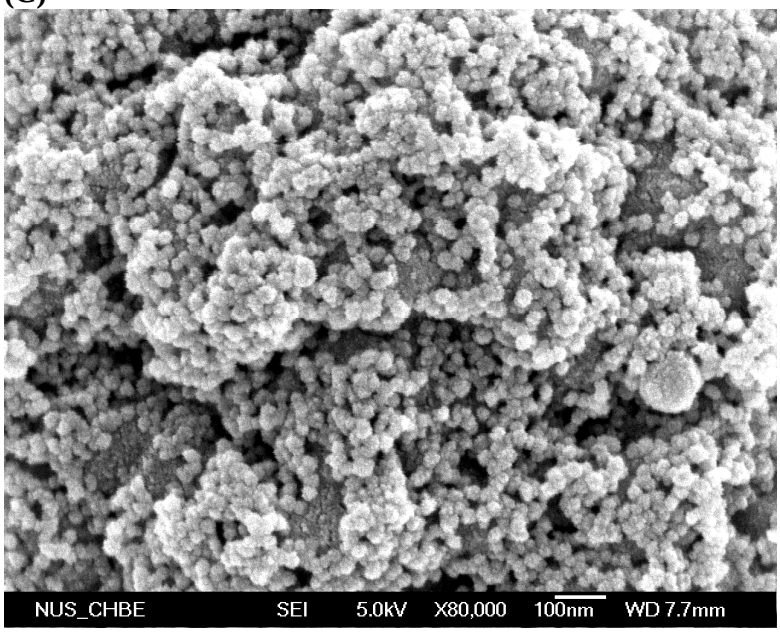

(D)

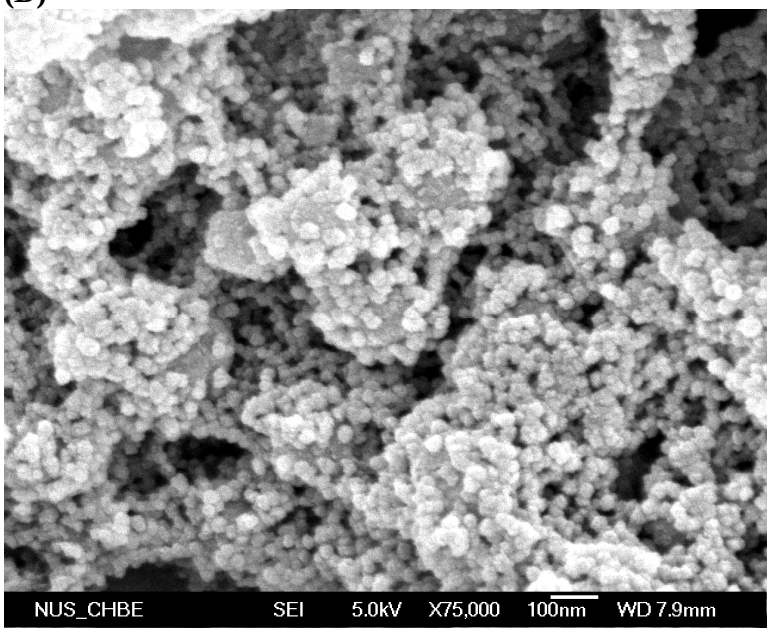

Figure 4.1 FESEM images of: (A) NIP, (B) BMIP, (C) RMIP, and (D) LMIP.

4.3.2 Elemental analysis

As mentioned in earlier, one of the main challenges in protein imprinting is the complete removal of the bulky template protein molecule from the polymer matrix after polymerisation, in order to vacate the binding sites so that they will be available for the subsequent rebinding with the target molecules. To demonstrate that the imprinted protein molecules were totally removed from the MIP's surface after the extensive washing steps, elemental analysis was carried out on the RMIP before and after washing, and using NIP as a control. The results from the elemental analysis (Table 4.2) showed that the protein was completely removed after the washing.

Polymer	**N composition (w%)**
NIP (before removal)	0*
NIP (after removal)	0*
RMIP (before removal)	0.659
RMIP (after removal)	0*

*Table 4.2 Results of the Elemental Analysis. *Below the detection limit of the elemental analyser.*

4.3.3 Batch rebinding tests

Batch rebinding tests involving single protein solutions were carried out on the imprinted (MIP) and the non-imprinted particles (NIP) to demonstrate whether molecular recognition has been achieved. In Figure 4.2A, batch rebinding tests at various initial RNase A concentrations were carried out (0.8-1.6 mg/ml) and by comparing the amount of

RNase A adsorbed by the RMIP and the NIP, it can be clearly seen that the RNase A-imprinted particles display a preferential uptake of RNase A. On the other hand, the other imprinted particles, BMIP and LMIP, did not exhibit any preference for the RNase A relative to the NIP. This demonstrated that molecular recognition for RNase A was imparted only to the RMIP during the miniemulsion polymerisation. Additionally, higher protein loadings for the RMIP were generally observed at higher initial protein concentrations. Figure 4.2B shows the results for the rebinding of the 4 types of particles with BSA solutions at various initial concentrations. Looking at the amount of adsorbed protein by the BMIP and NIP, it came as a surprise that the BSA-imprinted particles did not display any preferential binding to the BSA and in fact, the NIP displayed a much higher BSA uptake. Furthermore, the BSA loading by the BMIP were much less (<2 µmol/g) than the RNase A loading by the RMIP (10-60 µmol/g) in the previous batch rebinding test. This result is consistent with those from the previous chapter. This may be due to the fact that BSA is a much larger molecule than RNase A. Like previously, higher protein loadings were observed for BMIP at a higher initial protein concentration. Lys batch rebinding test was then carried out with LMIP and NIP at 3 initial Lys concentrations (Figure 4.2C). Even though the LMIP displayed higher averaged Lys loadings than the NIP, the difference was not statistically significant.

(A)

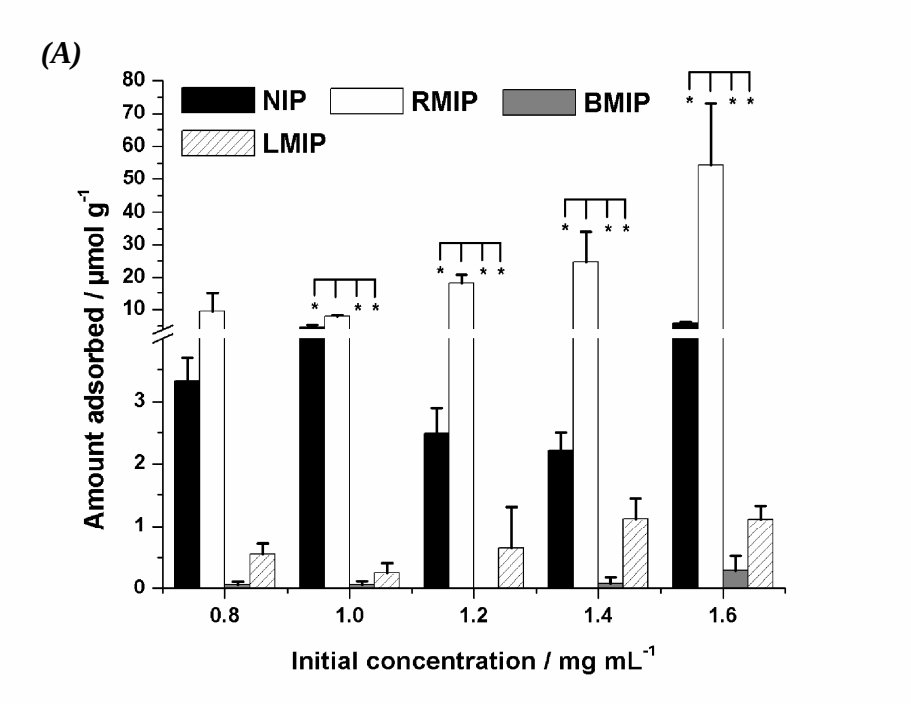
NIP
RMIP
BMIP
LMIP
Amount adsorbed / µmol g-1
Initial concentration / mg mL-1
0.8
1.0
1.2
1.4
1.6

(B)

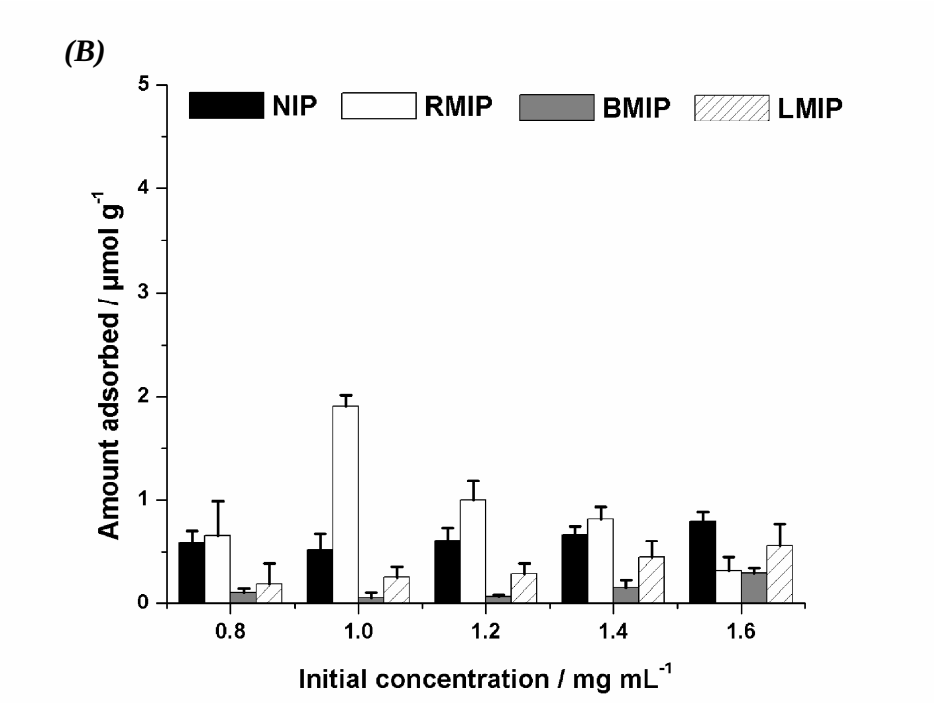
NIP
RMIP
BMIP
LMIP
Amount adsorbed / µmol g-1
Initial concentration / mg mL-1
0.8
1.0
1.2
1.4
1.6

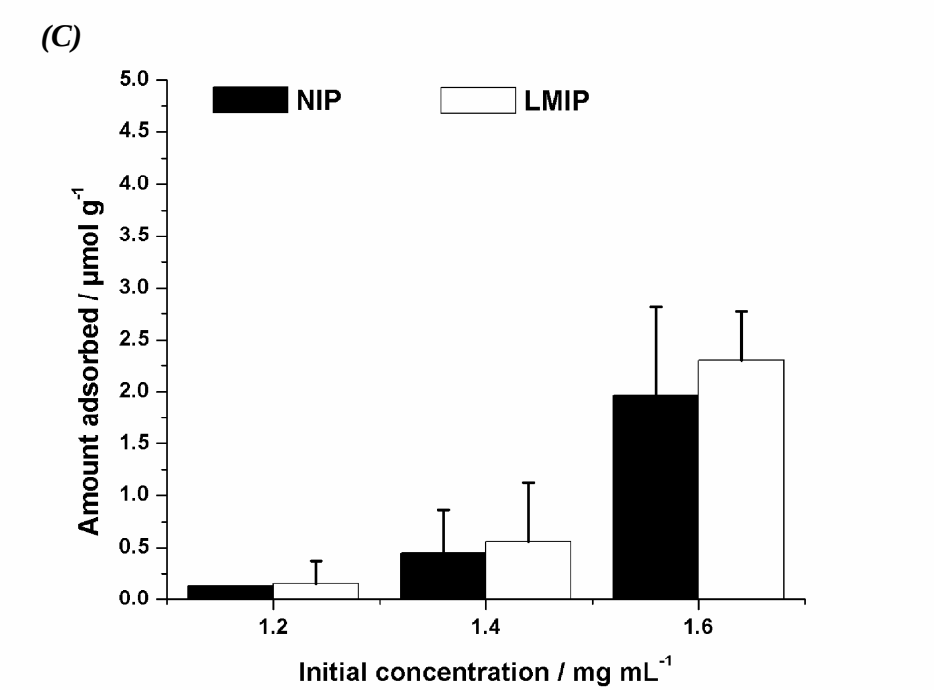

Figure 4.2 Results of batch rebinding tests in: (A) RNase A, (B) BSA, and (C) Lys protein solutions. Statistical significance (*) was determined using one-way ANOVA with Tukey HSD post hoc analysis with $p < 0.01$.

4.3.4 Competitive batch rebinding tests

The particles were subjected to rebinding tests in the presence of more than one type of protein in order to investigate if the imprinted particles could exhibit specific recognition for the template protein in a competitive environment. Binary batch rebinding test was conducted on the RMIP and NIP using a rebinding solution containing RNase A and BSA (both at an initial concentration of 1.2 mg/ml) and the results are displayed in Figure 4.3. The RNase A and BSA loadings on the NIP were 1.205 and 0.394 µmol protein/g NIP, respectively. The NIP and RMIP particles displayed similar BSA loading (0.412 µmol RNase A/g polymer) but there was a significant increase of about 80% in the RNase A loading between the two. This was expected since the RMIP had already exhibited

excellent molecular recognition for RNase A in the previous single protein batch rebinding test. The comparable BSA loadings between the 2 sets of particles could be attributed to non-specific binding of the BSA molecules on the surface of the particles. The static distribution coefficient, K_D, the separation factor, α, and the relative separation factor, β, for the RMIP and NIP were calculated and displayed in Table 4.3. The RMIP has a separation factor nearly twice as large as the NIP and this is another demonstration that molecular imprinting has been successfully achieved.

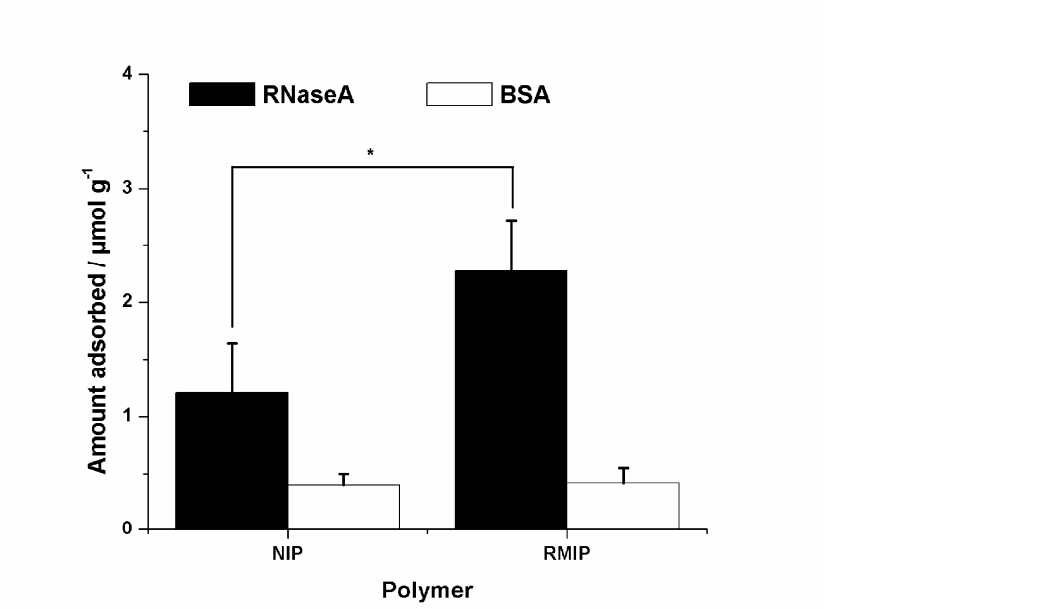

*Figure 4.3 Results of the binary protein competitive batch rebinding test. Student's t-test, *: p < 0.12.*

	RNase A		BSA		K_{D1} (ml/g)	K_{D2} (ml/g)	α	β
	C_p (µmol/g)	C_s (µmol/ml)	C_p (µmol/g)	C_s (µmol/ml)				
RMIP	2.268	0.08569	0.4124	0.01783	26.5	23.1	1.147	1.82
NIP	1.205	0.08642	0.3935	0.01780	13.9	22.1	0.630	-

Table 4.3 Calculated separation factors of the NIP and RMIP nanoparticles based on the competitive binary rebinding test.

Another batch rebinding test was carried out on all the particles in a more competitive environment where 3 proteins were present in the rebinding solution at an initial concentration of 1.8 mg/ml for each protein (Figure 4.4). The presence of 2 additional proteins competing for adsorption on the surface of the particle has caused the protein loadings to be limited to less than 1.6 µmol/g. The RMIP, like before, has a higher RNase A loading than the NIP but the specific recognition for RNase A was less pronounced, as expected in a much more competitive environment than the single and binary protein batch rebinding tests. The BMIP did not exhibit any preferential binding towards BSA relative to the NIP, which is consistent with the results from the earlier batch rebinding test. The LMIP displayed a higher average Lys loading than the NIP but the difference was not statistically significant. Taking into account the results from the above rebinding tests (single, binary, and ternary) conducted on the nanoparticles, it could be concluded that molecular imprinting was successfully achieve for the RMIP, whereas the LMIP and BMIP displayed only limited and no recognition for the template protein, respectively. It is interesting to note that the RNase A loading for the LMIP was higher than that for the RMIP in the ternary batch rebinding test. The exact reason for this result is not known but

the explanation could perhaps be found in the discussion of the imprinting mechanism in the latter part of this chapter.

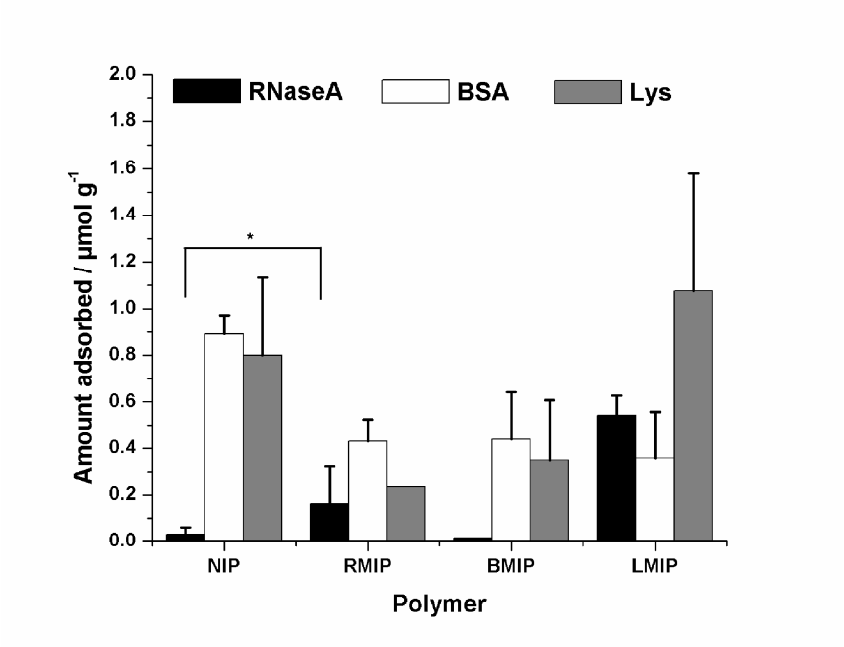

*Figure 4.4 Results of the ternary protein competitive batch rebinding test. Student's t-test, *: $p < 0.06$.*

4.3.5 Rebinding kinetics

One of the challenges in protein imprinting is the slow rebinding kinetics due to the large and bulky size of the protein molecules and their difficulty in reaching the imprinted binding sites. The miniemulsion polymerisation approach in this work has reduced this problem by producing imprinted nanoparticles with large specific surface areas and binding cavities which were located at the surface of the particles. A rebinding kinetics study was thus carried out on the RMIP and NIP in order to verify this. The rebinding profiles of the RMIP and NIP were generally very similar (Figure 4.5). In the first 150 minute, the RMIP exhibited a high rate of adsorption and up to 80% of the maximum

adsorption was achieved. The adsorption then slowed down significantly and equilibrium was reached approximately 100 minutes later. At the beginning of the kinetics rebinding test, all the binding sites on the imprinted nanoparticles were readily available and the protein was adsorbed at a high rate. As more binding sites were occupied, the adsorption rate decreased significantly until equilibrium is reached. The rebinding profile and the time to reach equilibrium are similar to the ones reported by Pang et al. (2006) and Fu et al. (2007). The imprinted nanoparticles which were synthesised in this work displayed favourable rebinding kinetics and, thus, are suitable for suitable for applications in the areas of analytical chemistry, biosensors, and separations.

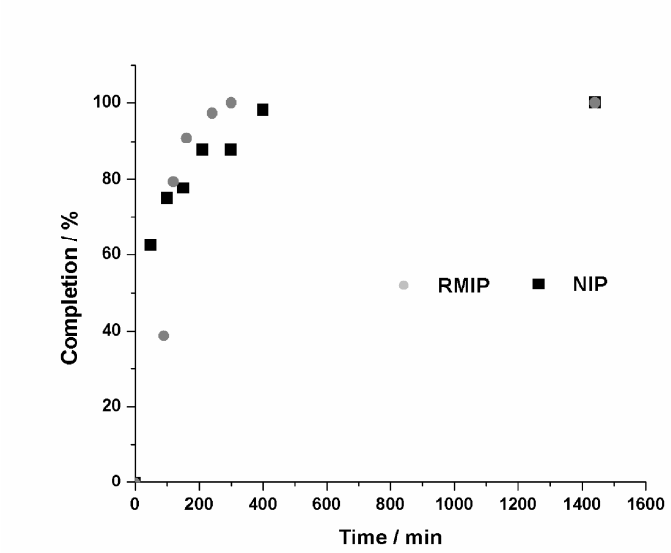

Figure 4.5 RNase A adsorption profiles of the NIP and RMIP nanoparticles.

4.3.6 Desorption study

Imprinted polymers have many advantages when compared to the traditional synthetic biomolecule-based molecular recognition techniques. They are able to withstand various

conditions and are able to be reused many times with no or little loss of affinity for the target molecule, making them economically preferable. In this section, a preliminary study was carried out on the RMIP in order to investigate its desorption ability after it has been subjected to rebinding with RNase A. The results would also provide a better insight into the type of bonding involved between the RMIP and the protein. Two solvents with different non-polarity were used and the results are displayed in Table 4.4. Initially, water was used as a solvent but only 38% of the RNase A was desorbed. However, this value increased to 62.3% when a solution of water and acetonitrile (in equal amounts) was used. Water was not effective in desorbing the protein and thus, in can be inferred that hydrogen bonding did not play an important part in the interaction between the protein and RMIP. When acetonitrile was added, the hydrophobicity of the solvent was increased and more protein was desorbed. This shows that the interactions involved in the uptake of the protein were hydrophobic and non-polar solvents will be more effective in removing the adsorbed protein. However, depending on the application, the correct solvent must be chosen with care in order to prevent the protein from being denatured as well as to preserve the imprinted particles for reuse.

Solvent	**Amount of RNase A desorbed (%)**
Water	38.0
Water:ACN (1:1)	62.3

Table 4.4 Results of the desorption study using different solvents.

4.3.7 Protein-surfactant interactions and their effects on the imprinting efficiency

In this work, spherical, highly monodispersed nanoparticles have been synthesised via miniemulsion polymerisation and molecular imprinting was carried out for 3 different template proteins. When RNase A was used as the template, the RMIP displayed excellent specific recognition for the template. However, when Lys and BSA were used as alternative templates, the LMIP exhibited only limited molecular recognition, whereas the BMIP showed no recognition for the template. In this section of the report, we will investigate the reason why molecular imprinting was not achieved with relative success when Lys and BSA were used as the template protein. It is hypothesised that the interaction between the protein molecules and the surfactant micellar system plays an important role in the success of protein imprinting. It was proposed by Moore et al. (2003) in his work on surfactant-protein interactions that in an aqueous solution, dissolved proteins tend to bind onto the surfactant micelles. From this, we can propose a mechanism which takes place during the imprinting of proteins via miniemulsion polymerisation. When the template protein is added to the pre-polymerisation mixture, the protein molecules bind onto the surfactant micelle containing the monomers and are partitioned across the boundary of the oil and water phases. This is possible because protein is a flexible molecule containing both hydrophobic and hydrophilic moieties. Polymerisation is then in carried out with the protein molecules trapped on the surface of the monomer-encapsulated micelles. Following the completion of the polymerisation, the removal of the template protein leaves a hydrophobic cavity complementary to the shape of the template protein. During the subsequent rebinding, the template protein preferentially binds via hydrophobic interactions to the shape-complementary site on the surface of the

nanoparticle (Figure 4.6). Hydrophobic interactions, coupled with a binding site which complements the shape of the protein molecule, provide a suitable bonding for molecular imprinting in an aqueous environment.

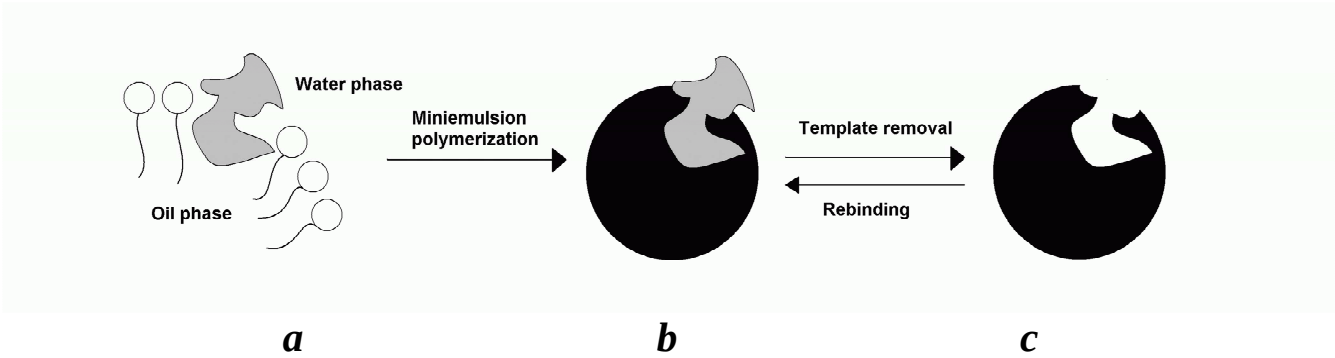

Figure 4.6 (a) Adsorption of template protein molecule to the micelle; (b) molecular imprinting on the surface of the nanoparticles; (c) removal of the template RNase A molecules frees the imprinted cavities.

However, surfactants are known for their denaturing effects on proteins and cause them to lose their native conformations. It is vital for a successful imprinting that the protein molecules preserve their native conformation in order to prevent the wrong 'shape' from being imprinted. This is important since proteins are molecules which are large and flexible. As a result, we have carried out an investigation using CD spectropolarimetry to study the effects of the surfactant solution used in the miniemulsion on the conformations of the 3 different types of protein. Figure 4.7 shows the spectra of the BSA in deionised water and two surfactant solutions: SDS and SDS/PVA. The native BSA spectrum (without any surfactant) shows two negative signals at 209 and 222 nm, characteristic of the absorption by the α-helices of the BSA. However, when either SDS or SDS/PVA was added, there was no significant difference in the CD spectra. The conformation of the BSA was thus preserved despite the addition of surfactant and it can be deduced that the

interactions between the surfactant and the BSA were limited. In a paper published by Ding et al. (2007), it was proposed that the interactions between SDS and BSA occurred in various steps with increasing surfactant concentration. At low SDS concentrations, individual SDS molecules bind to the protein via ionic and hydrophobic interactions but do not cause denaturation. When the concentration is increased, more SDS molecules bind to the protein and begin to cause conformational changes on the protein. Micelle-like clusters are also formed between the SDS monomers and the protein. When the concentration increases to the critical micelle concentration (CMC), most of the protein is fully denatured. The interaction between SDS and BSA is thus, a stepwise process (Takeda et al., 1987). In our protocol, the BSA was added directly to the SDS/PVA surfactant system (at a concentration above the CMC) and this prevented the surfactant from interacting with the BSA in a step-wise manner as described above. The initial complexation between the SDS monomers and the protein which aids the unfolding of the protein did not take place and it may have been difficult for the BSA to interact directly with the surfactant micelles. As a result, the surfactant-protein interaction was limited causing the BSA to remain in its native conformation.

The electrical charge on the protein could also provide a plausible explanation for the lack of surfactant-protein interaction. The isoelectric point (pI) for BSA is 4.7 and this gives the protein a net negative charge when added to the pre-polymerisation solution which has a pH of about 7.2. As a result, the electrostatic repulsion between the anionic SDS surfactant and the negatively charged BSA would limit the interaction between the two species. From our hypothesis, it is proposed that for molecular imprinting to be achieved, a certain amount of interaction between the monomer-encapsulated surfactant micelle and

the template protein must occur. The lack of interaction between the BSA and the surfactant would prevent the BSA from being partitioned across the oil-water phase boundary and thus explain why molecular imprinting was not achieved for the BMIP nanoparticles, as reflected in the rebinding tests. This theory is also consistent with the results from rebinding tests of the RMIP and LMIP nanoparticles. The pIs of RNase A and Lys are 9.45 and 11.0, respectively, and this would give both of the proteins a net positive charge in the pre-polymerisation solution during the imprinting process. The resulting electrostatic attraction would then promote interaction between the surfactant micelle and the protein and thus, molecular imprinting is more likely to be achieved.

In contrast, the Lys showed extensive interactions with the surfactant and its conformation was modified to a large extent, as shown by the Lys spectra (Figure 4.8). In the near-UV region (Figure 8A), the tertiary structure of the Lys caused a positive 'head-and-shoulders' peaks at 290 nm (head), 283 nm, and 293.5 nm (shoulders) in the spectra of the native protein (Goux and Hooker, 1980). However, the peaks disappeared after the addition of surfactant, reflecting the unfolding of the protein. Denaturation was also observed in the far-UV region (Figure 4.8B), signalled by the deepening of the negative peak at around 235 nm. Lys interacted significantly with the surfactant causing its shape to be altered from its native form and therefore, the LMIP nanoparticles only achieved limited molecular selectivity. Furthermore, the loss of the Lys native conformation would have caused the "incorrect template" to be imprinted and this might have be the reason why the RNase A loading for the LMIP nanoparticles was higher than that for the RMIP nanoparticles in the ternary batch rebinding test. This explanation is made more likely by the fact that Lys is very similar in size and molecular weight to RNase A.

The CD spectra of the RNase A are shown in Figure 4.9. Despite the addition of the SDS and PVA surfactants, the RNase A spectra retains its original shape but the characteristic peak at 218 nm experiences a moderate 'red-shift'. In contrast to the BSA and Lys, which showed limited and extensive surfactant-protein interactions, the RNase achieved an optimal level of interaction with the surfactant allowing the RNase A to partition across the micelle interface and at the same time, preventing a large degree of protein unfolding. As a result, the RMIP nanoparticles exhibited a high selectivity for RNase A in the rebinding tests which were carried out previously.

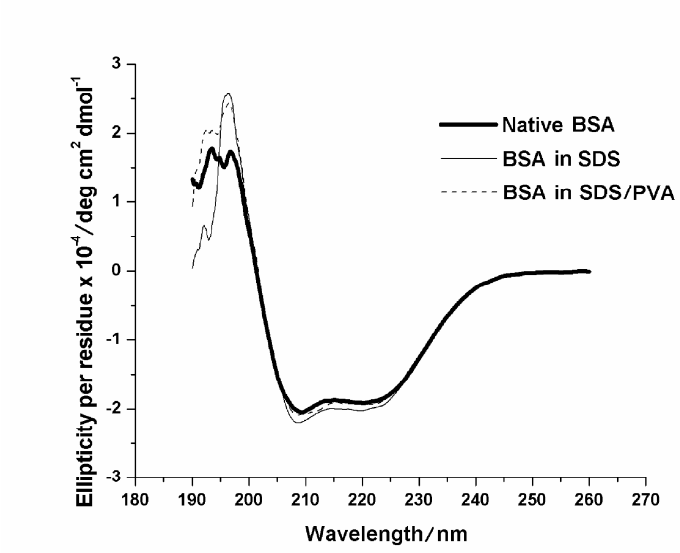

Figure 4.7 Solvent-corrected CD spectra of BSA in different types of surfactant systems, illustrating the lack of protein-surfactant interaction.

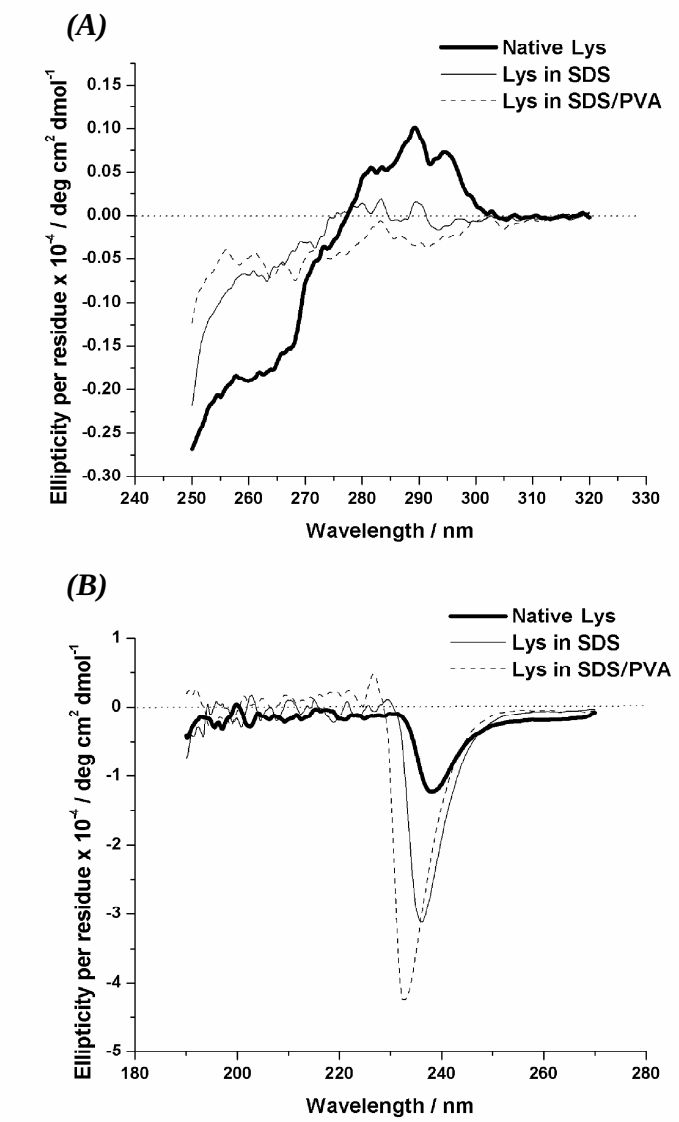

Figure 4.8 Solvent-corrected (A) near-UV and (B) far-UV CD spectra of Lys, illustrating the change in the protein structure in the presence of surfactants.

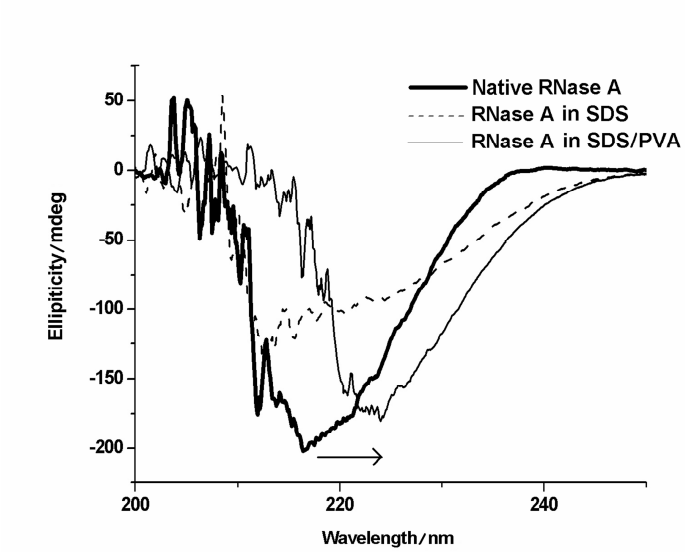

Figure 4.9 Solvent-corrected far-UV CD spectra of RNase A in surfactant solutions, illustrating an optimum level of protein-surfactant interaction for protein imprinting through miniemulsion polymerisation.

4.4 Conclusions

In this work, redox-initiated miniemulsion polymerisation was used to synthesise protein surface-imprinted nanoparticles following Tan's protocol. Three different proteins were chosen as the template: RNase A, Lys, and BSA. In the single- and multi-protein rebinding tests, the RMIP nanoparticles exhibited high molecular recognition for the RNase A with favourable rebinding kinetics. However, molecular selectivity was only modest for the LMIP nanoparticles and totally absent for the BMIP nanoparticles. In order to understand the results, further investigations were carried out using CD spectropolarimeter to observe the conformational changes experienced by the proteins in the SDS/PVA surfactant system which reflect the surfactant-protein interactions in the pre-polymerisation mixture. It was proposed that the interaction between the monomer-encapsulated surfactant micelles and the template protein plays an important role in the

imprinting process in the miniemulsion polymerisation system. An optimal protein-surfactant interaction must be achieved which is strong enough to allow the protein to be partitioned across the oil-water phase boundary but at the same time, not too extensive to prevent any drastic unfolding of the protein.

Chapter 5

Conclusions

In this research project, further investigations on Tan and Tong's protein imprinting work, which was published in 2007, have been carried out in order to obtain a deeper understanding of the imprinting process involved in their work. Tan had successfully synthesised uniform spherical nanoparticles with the ability to recognise and bind target protein molecules using molecular imprinting. A simple one-step miniemulsion polymerisation had been employed, with methyl methacrylate (MMA) and ethylene glycol dimethacrylate (EGDMA) as the functional monomer and the cross-linker, respectively. The use of the MMA had allowed molecular recognition to be achieved in an aqueous environment principally via hydrophobic interactions between the binding cavities on the imprinted particle surface and the protein molecules. In this final chapter, the findings and conclusions of the different investigations which were carried out in this research project are described. Furthermore, future investigations which could be carried out are also mentioned.

5.1 Determining the principal factors which affect the imprinting efficiency

The objective of this investigation was to optimise Tan's method and determine the principal factors and conditions which affect the ability of the imprinted nanoparticles to specifically recognise the target protein. Four batches of MIPs under different conditions

were synthesised using a modified protocol based on Tan's work using BSA as the template. Three different factors were chosen: the MMA:EGDMA ratio, the amount of BSA added, and the polymerisation temperature. The MIPs and NIPs synthesised were uniform and spherical with diameters ranging from 40 nm to 50 nm. Batch rebinding tests were carried out to test their imprinting efficiency but only one set of MIPs (condition T8) exhibited any molecular recognition for the target BSA and the optimisation analysis was not completed. At condition T8, the higher polymerisation temperature had increased the extent of polymerisation, decreasing the swelling ratio (SR) and improving the imprinting efficiency. The higher concentrations of the functional monomer and the template protein (MMA and BSA, respectively) had also improved the specific recognition of the MIP by increasing the extent of formation of binding sites on the MIP's surface.

5.2 Investigating protein-surfactant interactions and their role in successful imprinting

In Chapter 4, Tan's method was used without any modification to synthesise RNase A-, BSA, and Lys-imprinted nanoparticles. The resulting particles were of similar size as previously but had a much smaller SR. The RNase A-imprinted nanoparticles displayed excellent specific recognition, whereas the Lys- and BSA-imprinted nanoparticles displayed limited and no molecular selectivity, respectively. It was hypothesised that in the miniemulsion, the partitioning of the protein across the oil-water phase boundary of the monomer-encapsulated surfactant micelle was responsible for the creation of imprinted sites on the nanoparticles surface. As a result, CD spectropolarimetry analysis

was carried out to study the interactions between the proteins and the surfactant micelles. It was observed that the BSA experienced no conformational changes in the surfactant solution, reflecting the lack of interactions between the protein molecules and the surfactant micelles. In contrast, the Lys interacted significantly with the surfactant micelles and experienced a drastic change in conformation. It was concluded that the lack of surfactant-protein interaction was responsible for the failure of the BMIP nanoparticles to exhibit any molecular selectivity. However, a large degree of interaction would result in the lost of the protein's native conformation and cause the 'incorrect template' to be imprinted, as shown by the LMIP particles. An optimal interaction must be reached for molecular imprinting to be successful, as in the case of RMIP particles, so that the protein is partitioned across the oil-water interface without losing its native conformation.

5.3 Suggestions for future work

5.3.1 Further investigation on the protein-surfactant interaction

To confirm the results of the CD spectropolarimetry analysis, dynamic light scattering (DLS) measurements could also be used to study the size of the micelles in the presence of the proteins. An increase in the micelle's size would be expected when there is a large degree of interaction between the protein and surfactant micelles.

In Section 4.3.7, one of the possible explanations for the lack of interaction was the net electrical charge of the protein. This hypothesis could be tested by replacing the SDS,

which is an anionic surfactant, by a cationic surfactant (e.g. cetyl trimethylammonium bromide) and DLS could be used to observe the changes in the sizes of the micelles. BSA, being negatively charged at neutral pH, would interact more with CTAB than SDS, and conversely, lower interactions would be observed for Lys and RNase A.

5.3.2 Modification of the BSA to improve its interaction with the surfactant micelle

It was demonstrated in this research project that Tan's method for protein imprinting was only effective in synthesising imprinted nanoparticles when RNase A was chosen as the template protein. The failure of the BMIP particles to exhibit any molecular selectivity was attributed to the lack of interactions between the BSA molecules and the surfactant micelles. This interaction could be improved by increasing the hydrophobicity of the protein which in turn, would aid the partitioning of the protein across the oil-water phase boundary. Moderate chemical modifications of the BSA could be carried out to increase its hydrophobicity without altering its native conformation. BSA possesses a single sulphhydryl group (Cys-34) located near the surface of the protein which could be targeted for alkylation (Carter and Ho, 1994; Peters Jr., 1995). Haloacids and their amides readily alkylate the free cysteine residue in preference to the other functional groups in the protein and their reactions could be restricted largely or exclusively to the SH group under appropriate conditions, such as short reaction time and low excess reagent (Torchinskii, 1974).

Bibliography

Alvarez-Lorenzo, C. and A. Concheiro. 2004. Molecularly imprinted polymers for drug delivery. J. Chromatogr. B. 804:231-245.

Ansell, RJ., and K. Mosbach. 1997. Molecularly Imprinted Polymers by Suspension Polymerisation in Perfluorocarbon Liquids, with Emphasis on the Influence of the Porogenic Solvent. J. Chromatogr. A. 787:55-66.

Asua, JM. 2002. Miniemulsion polymerization. Prog. Polym. Sci. 27:1283-1346.

Bergmann, NM. and NA. Peppas. 2008. Molecularly imprinted polymers with specific recognition for macromolecules and proteins. Prog. Polym. Sci. 33:271-288.

Bonini, F., S. Piletsky, APF. Turner, A. Speghini and A. Bossi. 2007. Surface imprinted beads for the recognition of human serum albumin. Biosens. Bioelectron. 22:2322-2328.

Bossi, A., F. Bonini, APF. Turner and S. Piletsky. 2007. Molecularly imprinted polymers for the recognition of proteins: The state of the art. Biosens. Bioelectron. 22:1131-1137.

Bossi, A., SA. Piletsky, EV. Piletska, PG. Righetti and APF. Turner. 2001. Surface-grafted molecularly imprinted polymers for protein recognition. Anal. Chem. 73:5281-5286.

Carter, DC. and JX. Ho. 1994. Structure of serum albumin. Adv. Protein Chem. 45:153-203.

Chen, MC. and RC. Lord. 1976. Laser Raman spectroscopic studies of the thermal unfolding of ribonuclease A. Biochemistry.15:1889-97.

Chou, PC., J. Rick and TC. Chou. 2005. C-reactive protein thin-film molecularly imprinted polymers formed using a micro-contact approach. Anal. Chim. Acta. 542:20-25.

Cormack, PAG. and AZ. Elorza. 2004. Molecularly imprinted polymers: synthesis and characterisation. J. Chromatogr. B. 804:173-182.

Dickert, FL., O. Hayden, and KP. Halikias. 2001. Synthetic receptors as sensor coatings for molecules and living cells. The Analyst. 126:760-771.

Ding, Y., Y. Shu, L. Ge and R. Guo. 2007. The effect of sodium dodecyl sulfate on the conformation of bovine serum albumin. Colloid Surface A. 298:163-169.

El-Toufaili, FA., A. Visnjevski and O. Bruggemann. 2004. Screening combinatorial libraries of molecularly imprinted polymer films casted on membranes in single-use membrane modules. J. Chromatogr. B. 804:135-139.

Fish, WP., J. Ferreira, RD. Sheardy, NH. Snow and TP. O'Brien. 2005. Rational design of an imprinted polymer: Maximizing selectivity by optimizing the monomer-template ratio for a cinchonidine MIP, prior to polymerization, using microcalorimetry. J. Liq. Chromatogr. Related Technol. 28:1-15.

Flores, A., D. Cunliff, MJ. Whitcombe and EN. Vulfson. 2000. Imprinted polymers prepared by aqueous suspension polymerization. J. Appl. Polym. Sci. 77:1841-1850.

Fu, GQ., JC. Zhao, H. Yu, L. Liu and BL. He. 2007. Bovine serum albumin-imprinted polymer gels prepared by graft copolymerization of acrylamide on chitosan. React. Funct. Polym. 67:442-450.

Furlong, NE. Research methods and statistics: an integrated approach. Wadsworth Publishing. 1999.

Gai, Q., Q. Liu, X. He, W. Li, L. Chen and Y. Zhang. 2008. Molecular imprinting technology for protein recognition. Prog. Chem. 20:957-968.

Guo, TY., YQ. Xia, J. Wang, MD. Song and BH. Zhang. 2005. Chitosan beads as molecularly imprinted polymer matrix for selective separation of proteins. Biomaterials. 26:5737-5745.

Hayden, O. and FL. Dickert. 2001. Selective microorganism detection with cell surface imprinted polymers. Adv. Mater. 13:1480-1483.

Hayden, O., PA. Lieberzeit, D. Blaas and FL. Dickert. 2006. Artificial antibodies for bioanalyte detection-sensing viruses and proteins. Adv. Funct. Mater. 16:1269-1278.

Hillberg, AL., K.R. Brain and CJ. Allender. 2005. Molecular imprinted polymer sensors: Implications for therapeutics. Adv. Drug Delivery Rev. 57:1875-1889.

Hiratani, H., A. Fujiwara, Y. Tamiya, Y. Mizutani and C. Alvarez-Lorenzo. 2005. Ocular release of timolol from molecularly imprinted soft contact lenses. Biomaterials. 26:1293-1298.

Hirayama, K., Y. Sakai and K. Kameoka. 2001. Synthesis of polymer particles with specific lysozyme recognition sites by a molecular imprinting technique. J. Appl. Polym. Sci. 81:3378-3387.

Janiak, DS. and P. Kofinas. 2007. Molecular imprinting of peptides and proteins in aqueous media. Anal. Bioanal. Chem. 389:399-404.

Kandimalla, VB. and HX. Ju. 2004. Molecular imprinting: a dynamic technique for diverse applications in analytical chemistry. Anal. Bioanal. Chem. 380:587-605.

Kempe, M., M. Glad, and K. Mosbach. 1995. An approach towards surface imprinting using the enzyme Ribonuclease A. J. Mol. Recogn. 8:35-39.

Kempe, H. and M. Kempe. 2006. Development and evaluation of spherical molecularly imprinted polymer beads. Anal. Chem. 78:3659-3666.

Kempe, M., and K. Mosbach. 1995. Separation of amino acids, peptides and proteins on molecularly imprinted stationary phases. J. Chromatogr. A. 691:317-323.

Kuehl, RO. Statistical principles of research design and analysis. Duxbury Pr: Book&Disk edition. 1994.

Lu, SL., G.X. Cheng and XS. Pang. 2003. Preparation of molecularly imprinted Fe3O4/P(St-DVB) composite beads with magnetic susceptibility and their characteristics of molecular recognition for amino acid. J. Appl. Polym. Sci. 89:3790-3796.

Lu, SL., GX. Cheng and XS. Pang. 2006. Study on preparation of protein-imprinted soft-wet gel composite microspheres with magnetic susceptibility and their characteristics. J. Appl. Polym. Sci. 100:684-694.

Mahony, JO., K. Nolan, MR. Smyth and B. Mizaikoff. 2005. Molecularly imprinted polymers-potential and challenges in analytical chemistry. Anal. Chim. Acta. 534:31-39.

Mayes, AG., LI. Andersson, and K. Mosbach. 1994. Sugar binding polymers showing high anomeric and epimeric discrimination obtained by non-covalent molecular imprinting. Anal. Biochem. 222:483-488.

Mayes, AG. and K. Mosbach. 1996. Molecularly imprinted polymer beads: Suspension polymerization using a liquid perfluorocarbon as the dispersing phase. Anal. Chem. 68:3769-3774.

Mitchell, ML. Research design explained. Wadsworth Publishing: 4th edition. 2001.

Miyahara, T. and K. Kurihara. 2000. Two-dimensional molecular imprinting: Binding of sugars to boronic acid functionalised, polymerised Langmuir-Blodgett films. Chem. Lett. 29:1356-1357.

Moore, PN., Puvvada S. and Blankschtein D. 2003. Role of the Surfactant Polar Head Structure in Protein−Surfactant Complexation: Zein Protein Solubilization by SDS and by SDS/C12En Surfactant Solutions. Langmuir. 19:1009-1016.

Nagarajan, R. 2001. Surfactant-Polymer Interactions. In New Horizons: Detergents for the New Millenium Conference. American Oil Chemists Society and Consumer Specialty Products Association. Port Myers, Florida.

Nicholls, IA., LI. Andersson, K. Mosbach, and B. Ekberg. 1995. Recognition and enantioselection of drugs and biochemicals using molecularly imprinted polymer technology. Trends Biotechnol. 13:47-51.

Nicholls, IA. and JP. Rosengren. 2001. Molecular imprinting of surfaces. Bioseparation. 10:301-305.

Pang, X.S., GX. Cheng, RS. Li, SL. Lu and YH. Zhang. 2005. Bovine serum albumin-imprinted polyacrylamide gel beads prepared via inverse-phase seed suspension polymerization. Anal. Chim. Acta. 550:13-17

Pang, XS., GX. Cheng, SL. Lu and EJ. Tang. 2006. Synthesis of polyacrylamide gel beads with electrostatic functional groups for the molecular imprinting of bovine serum albumin. Anal. Bioanal. Chem. 384:225-230.

Parmpi, P. and P. Kofinas. 2004. Biomimetic glucose recognition using molecularly imprinted polymer hydrogels. Biomaterials. 25:1969-1973.

Perez, N., MJ. Whitcombe and EN. Vulfson. 2000. Molecularly imprinted nanoparticles prepared by core-shell emulsion polymerization. J. Appl. Polym. Sci. 77:1851-1859.

Peters, T. Jr. All about albumin. Academic Press. 1995. pp. 54.

Piletsky, SA., A. Guerreiro, EV. Piletska, I. Chianella, K. Karim and APF. Turner. 2004. Polymer cookery. 2. Influence of polymerization pressure and polymer swelling on the performance of molecularly imprinted polymers. Macromolecules. 37:5018-5022.

Piletsky, SA., EV. Piletska, A. Bossi, K. Karim, P. Lowe and APF. Turner. 2001. Substitution of antibodies and receptors with molecularly imprinted polymers in enzyme-linked and fluorescent assays. Biosens. Bioelectron. 16:701-707.

Piletsky, SA., EV. Piletskaya, TA. Sergeyeva, TL. Panasyuk, and AV. El'skaya. 1999. Molecularly Imprinted Self-Assembled Films with Specificity to Cholesterol. Sens. Act. B. 60:216-220.

Poole, S., SI. West and JC. Fry. 1987. Effects of basic proteins on the denaturation and heat-gelation of acidic proteins. Food Hydrocolloids. 1:301-316.

Ramanaviciene, A. and A. Ramanavicius. 2004. Molecularly imprinted polypyrrole-based synthetic receptor for direct detection of bovine leukemia virus glycoproteins. Biosens. Bioelectron. 20:1076-1082.

Ramstrom, O. and RJ. Ansell. 1998. Molecular Imprinting Technology: Challenges and Prospects for the Future. Chirality. 10:195-209.

Ramström, O., L. Ye, M. Krook, and K. Mosbach. 1998. Applications of Molecularly Imprinted Materials as Selective Adsorbents: Emphasis on Enzymatic Equilibrium Shifting and Library Screening. Chromatographia. 47:465-469.

Rao, TP., R. Kala and S. Daniel. 2006. Metal ion-imprinted polymers - Novel materials for selective recognition of inorganics. Anal. Chim. Acta. 578:105-116.

Reddy, PS., T. Kobayashi, and N. Fujii. 1999. Molecular Imprinting in Hydrogen Bonding Networks of Polyamide Nylon for Recognition of Amino Acids. Chem. Lett. 4:193-194.

Say, R., E. Birlik, A. Ersoz, F. Yilmaz, T. Gedikbey and A. Denizli. 2003. Preconcentration of copper on ion-selective imprinted polymer microbeads. Anal. Chim. Acta. 480:251-258.

Sellergren, B. 2000. Imprinted polymers with memory for small molecules, proteins, or crystals. Angew. Chem. Intl. Ed. 39:1031-1039.

Sellergren, B. (Ed.). Molecularly Imprinted Polymers: Man-made mimics of antibodies and their applications in analytical chemistry, Techniques and Instrumentation in Analytical Chemistry, Vol.23. Elsevier Science: Amsterdam. 2001. pp. 74, 167.

Sergeyeva, TA., SA. Piletsky, EV. Piletska, OO. Brovko, LV. Karabanova, LM. Sergeeva, AV. El'skaya and APF. Turner. 2003. In situ formation of porous molecularly imprinted polymer membranes, Macromolecules. 36:7352-7357.

Shi, HQ., WB. Tsai, MD. Garrison, S. Ferrari, and BD. Ratner. 1999. Template-Imprinted Nanostructured Surfaces for Protein Recognition. Nature. 398:593-597.

Shiomi, T., M. Matsui, F. Mizukami and K. Sakaguchi. 2005. A method for the molecular imprinting of hemoglobin on silica surfaces using silanes. Biomaterials. 26:5564-5571.

Shirvani-Arani, S., SJ. Ahmadi, A. Bahrami-Samani, and M. Ghannadi-Maragheh. 2008. Synthesis of nano-pore samarium (III)-imprinted polymer for preconcentrative separation

of samarium ions from other lanthanide ions via solid phase extraction. Anal. Chim. Acta. 623:82-88.

Sineriz, F., Y. Ikeda, E. Petit, L. Bultel, K. Haupt, J. Kovensky and D. Papy-Garcia. 2007. Towards an alternative for specific recognition of sulfated sugars. Preparation of highly specific molecular imprinted polymers. Tetrahedron. 63:1857-1862.

Smyth, DG., WH. Stein and S. Moore. 1963. The sequence of amino acid residues in bovine pancreatic ribonuclease. J. Biol. Chem. 238:227–234.

Stelea, SD., P. Pancoska, AS. Benight and TA. Keiderling. 2001. Thermal unfolding of ribonuclease A in phosphate at neutral pH: Deviations from the two-state model. Protein Sci. 10:970-978.

Takeda, K., M. Shigeta and K. Aoki. 1987. Secondary structures of bovine serum albumin in anionic and cationic surfactant solutions. Colloid Interface Sci. 117:120-126.

Takeuchi, T., and J. Haginaka. 1999. Separation and Sensing Based on Molecular Recognition Using Molecularly Imprinted Polymers. J. Chromatogr. B. 728:1-20.

Tan, CJ. and YW. Tong. 2007a. The effect of protein structural conformation on nanoparticle molecular imprinting of ribonuclease A using miniemulsion polymerisation. Langmuir. 23:2722-2730.

Tan, C.J. and YW. Tong. 2007b. Molecularly imprinted beads by surface imprinting. Anal. Bioanal. Chem. 389:369-376.

Torchinskii, Y.M.. Sulfhydryl and disulfide groups of proteins. Consultants Bureau: New York. 1974. pp. 34.

Turner, NW., CW. Jeans, KR. Brain, CJ. Allender, V. Hlady and DW. Britt. 2006. From 3D to 2D: A review of the molecular imprinting of proteins. Biotechnol. Prog. 22:1474-1489.

Turner, NW., X. Liu, SA. Piletsky, V. Hlady and DW. Britt. 2007. Recognition of conformational changes in, beta-lactoglobulin by molecularly imprinted thin films. Biomacromolecules. 8:2781-2787.

Vaihinger, D., K. Landfester, I. Krauter, H. Brunner and GEM. Tovar. 2002. Molecularly imprinted polymer nanospheres as synthetic affinity receptors obtained by miniemulsion polymerisation. Macromol. Chem. Phys. 203:1965-1973.

Whitcombe, MJ., ME. Rodriguez, P. Villar, and EN. Vulfson. 1995. A new method for the introduction of recognition site functionality into polymers prepared by molecular imprinting: Synthesis and characterization of polymeric receptors for cholesterol. J. Am. Chem. Soc. 117:7105-7111.

Whitcombe, MJ. and EN. Vulfson. 2001. Imprinted polymers. Adv. Mater. 13:467

Wulff, G. 2002. Enzyme-like catalysis by molecularly imprinted polymers. Chem. Rev. 102:1-27.

Yan, CL., Y. Lu and SY. Gao. 2007. Coating lysozyme molecularly imprinted thin films on the surface of microspheres in aqueous solutions. J. Polym. Sci., Part A: Polym. Chem. 45:1911-1919.

Ye, L. and K. Haupt. 2004. Molecularly imprinted polymers as antibody and receptor mimics for assays, sensors and drug discovery. Anal. Bioanal. Chem. 378:1887-1897.

Ye, L. and K. Mosbach. 2008. Molecular imprinting: Synthetic materials as substitutes for biological antibodies and receptors. Chem. Mater. 20:859-868.

Yilmaz, E., K. Haupt and K. Mosbach. 2000. The use of immobilized templates - A new approach in molecular imprinting. Angew. Chem.-Int. Edit. 39:2115

Yoshida, M., K. Uezu, M. Goto, and S. Furusaki. 1999. Metal Ion Imprinted Microsphere Prepared by Surface Molecular Imprinting Technique Using Water-in-Oil-Water Emulsions. J. Appl. Polym. Sci. 73:1223-1230.

Zhang, HQ., L. Ye and K. Mosbach. 2006. Non-covalent molecular imprinting with emphasis on its application in separation and drug development. J. Mol. Recognit. 19:248-259.

Zhu, XL., and QS. Zhu. 2008. Molecular imprinted Nylon-6 stir bar as a novel extraction technique for enantioseparation of amino acids. J. Appl. Polym. Sci. 109:2665-2670.

Appendix A

List of publications

Journal publications

Tan, C.J., S. Wangrangsimakul, R. Bai and Y.W. Tong. 2008. Defining the interactions between proteins and surfactants for nanoparticle surface imprinting through miniemulsion. Chem. Mater. 20:118-127.

Tan, C.J., S. Wangrangsimakul, N. Sankarakumar and Y.W. Tong. 2008. Response to comment on “Preparation of Superparamagnetic Ribonuclease A Surface-Imprinted Submicrometer Particles for Protein Recognition in Aqueous Media”. Anal. Chem. 80:9375-9376.